RNA aptamer delivery through intact human skin

Jon D. Lenn[1], Jessica Neil[1], Christine Donahue[2], Kellie Demock[2], Caitlin Vestal Tibbetts[2], Javier Cote-Sierra[3], Susan H. Smith[4], David Rubenstein[4], Jean-Philippe Therrien[4], P. Shannon Pendergrast[5], Jason Killough[6], Marc B. Brown[7], Adrian C. Williams[8]

1) MedPharm; RTP, NC; 2) GlaxoSmithKline, R&D Platform Technology & Science, Waltham, MA; 3) Pfizer, Worldwide Research & Development; 4) GlaxoSmithKline, Center For Skin Biology; RTP, NC; 5) Ymir Genomics, Cambridge MA; 6) Momenta Pharmaceuticals, Cambridge MA; 7) Honorary Professor at University of Reading and CSO MedPharm Ltd 8) Professor of Pharmaceutics, School of Pharmacy; University of Reading

ORCID:

A.C. Williams: 0000-0003-3654-7916

Work was primarily performed in Research Triangle Park, Raleigh, North Carolina, USA.

Corresponding author:

Dr Jon Lenn

VP US Operations, MedPharm

Durham,

North Carolina

jon.lenn@medpharm.co.uk

Tel: 919-450-5673

ABBREVIATIONS: SC, stratum corneum; mAb, monoclonal antibody; log $P_{(oct/water)}$, log partition coefficient between octanol and water; SELEX, Systematic evolution of ligands by exponential enrichment; STAT, signal transducer and activator of transcription; dAb, domain antibody

ABSTRACT

It is generally recognised that only relatively small molecular weight (typically < ~500 Da) drugs can effectively permeate through intact stratum corneum. Here, we challenge this orthodoxy using a 62-nucleotide (MW=20,395) RNA-based aptamer, highly specific to the human IL-23 cytokine, with picomolar activity. Results demonstrate penetration of the aptamer into freshly excised human skin using two different fluorescent labels. A dual hybridisation assay quantified aptamer from the epidermis and dermis giving levels far exceeding the cellular IC_{50} values (> 100,000-fold) and aptamer integrity was confirmed using an oligonucleotide precipitation assay. A Th17 response was stimulated in freshly excised human skin resulting in significantly upregulated IL-17f, and 22; topical application of the IL-23 aptamer decreased both IL-17f and IL-22 by approximately 45% but did not result in significant changes to IL-23 mRNA levels, confirming that the aptamer did not globally suppress mRNA levels. This study demonstrates that very large molecular weight RNA aptamers can permeate across the intact human skin barrier to therapeutically relevant levels into both the epidermis and dermis and that the skin penetrating aptamer retains its biologically active conformational structure capable of binding to endogenous IL-23.

INTRODUCTION

It is widely accepted that the intact stratum corneum (SC) provides the primary barrier to topical and transdermal drug delivery and so restricts the therapeutic targets that can be accessed topically. Relatively few molecules have the appropriate physicochemical and therapeutic properties to allow topical and transdermal administration. It is generally recognised that only relatively small molecular weight (typically <500 Da) and moderately lipophilic (log $P_{(oct/water)}$ 1-3.5) drugs can effectively permeate through the SC (Bos and Meinardi, 2000; Williams, 2003).

The introduction of biological therapeutic agents has revolutionised the treatment of psoriasis, a chronic inflammatory skin disorder. Although effective when delivered systemically, the large size of proteins, including monoclonal antibodies, domain antibodies, and even Fab fragments, is thought to preclude their development as topical medicines. Aptamers are oligonucleotide-based molecules that can specifically bind to proteins or other cellular targets; aptamers have been approved for macular degeneration, and others are in clinical development for cancer, haemophilia, anaemia, and diabetes (Darisipudi et al, 2011; Ng et al, 2006; Parunov et al, 2011; Schwoebel et al, 2013). Aptamers offer a significant advantage over antisense molecules because their structure and composition can be modified while retaining pharmacological activity and they possess conformational plasticity and flexibility (Nomura et al, 2010). Systematic evolution of ligands by exponential enrichment (SELEX) has accelerated the discovery and development of aptamers allowing functional isolation of oligonucleotides against specific targets that could be used to treat skin diseases (Keefe et al, 2010).

Psoriasis is driven by activated T cells (Di Cesare et al, 2009). Elevated levels of IL-23 and Th17-related cytokines in lesional skin biopsies encouraged targeting of the IL-23/Th17 pathway for psoriasis treatment (Blauvelt, 2008). Ustekinumab, a human IgG1κ monoclonal antibody (mAb) that binds to the p40 protein subunit of IL-12 and IL-23 cytokines, is approved for moderate/severe plaque psoriasis. However, there are risks associated with long term systemic p40 inhibition given the role of IL-12 in intracellular microbial response and tumour suppression (Koutruba et al, 2010; Tausend et al, 2014). To circumvent this, a human mAb specifically directed against IL-23 gave positive clinical responses in patients with

moderate-to-severe psoriasis, suggesting that neutralizing IL-23 alone is a promising psoriasis therapy (Sofen et al, 2014).

We have developed and optimized an aptamer that is a first-in-class inhibitor of IL-23 for topical treatment of psoriasis (Figure 1). This water-soluble 62-nucleotide (MW=20,395) aptamer has high affinity and specificity to human IL-23 cytokine. Employing a well-validated model, it has been shown that, *without* physically disrupting the SC, this large molecular weight RNA based aptamer can penetrate into and permeate through human skin. Analyses to extract, detect and quantify the macromolecule in human skin showed the IL-23 aptamer was present at therapeutically relevant levels. Finally, delivery was confirmed through a cytokine induced inflammatory *ex vivo* human skin model (Smith, et al, 2016). This study shows the passive delivery of a large molecular weight aptamer across intact human skin.

RESULTS

The IL-23 aptamer is biologically active

Biological activity of the aptamer was confirmed in three different assays. Inhibition of IL-23 dependent stimulation of STAT3 activity in PHA-Blast cells showed that the 61-mer minimer (IC_{50} 0.075 nM ± 0.030 nM) was more potent than the parent full length (84-mer) IL-23 aptamer (IC_{50} 0.26 nM ± 0.036 nM); the activity of both aptamers was greater than the control anti-p19 antibody (IC_{50} 0.69 nM ± 0.12 nM). Secondly, the aptamer blocked endogenous IL-23 activation in PHA/IL-2 activated T-cells, evaluated by measuring levels of phospho-STAT3. Finally, the IL-23 aptamer did not inhibit IL-12 activation of PHA/IL-2 activated T-cells; many IL-23 antagonists also inhibit IL-12 since they share the p40 subunit but our IL-23 aptamer only inhibits IL-23 activation and not IL-12 activation, similar to the anti-p19 antibody. Experimental methods and representative inhibition curves can be found in Supplementary Information (S1).

The IL-23 aptamer penetrates human skin

Passive penetration of topically applied IL-23 (20.4 kDa) aptamer through human skin was assessed using freshly excised skin with and without a fully functional stratum corneum barrier (Figure 2a). Fluorescently labelled IL-23 aptamer (21.4 kDa) was formulated in an oil-in-water cream vehicle previously described to aid delivery of macromolecules (Mehta et al, 2000). A finite dose (10 mg/cm^2 of formulation containing 1% aptamer) was applied to

skin mounted in flow-through diffusion cells. To ensure the washing procedure effectively removed residual aptamer from the skin surface and to assess tissue auto fluorescence, the medicated cream was applied and immediately removed (zero hour sample). No fluorescence in intact or partially compromised skin confirmed the washing procedure effectively removed residual aptamer from the skin surface. Interestingly, skin with the SC removed allowed permeation at this zero hour sample suggesting the aptamer permeates through the viable epidermis almost immediately and is not further limited by tight junctions in the epidermis. In contrast, a single domain antibody (dAb) fragment (13.1 kDa) failed to permeate into the viable epidermis of tape stripped skin (Figure 2b) demonstrating that these junctions can regulate passive diffusion of large molecular weight biological agents. After four hours of topical exposure, the IL-23 aptamer penetrated not only fully and partially compromised tissue, but also through intact human skin, with an intensity gradient decreasing from the skin surface to the basement membrane. Interestingly, after dosing full thickness intact skin, no aptamer was detected in the receiver solution but rather the macromolecule appears to be retained in the tissue, perhaps via cellular uptake (see below).

To confirm that the aptamer indeed penetrated the skin and that fluorescence was not simply due to dissociation of the label, the IL-23 aptamer was extracted from non-compromised (Unt) and partially compromised (Abr) skin samples, visualized fluorescently on a polyacrylamide gel and compared to the IL-23 aptamer dylight 488 standard (IL-23 aptamer) and a 28-mer SDF-1 aptamer (28-mer) (Figure 2c). Concordance of skin extracted aptamer with the IL-23 aptamer dylight 488 standard shows delivery of intact labelled macromolecules to these skin layers, providing evidence that the fluorescence images are not from dissociation of the label though this cannot be fully discounted from the images in (a) and (b) alone.

Delivery into intact human abdominal skin with longer exposures using a second fluorescent label (Cy3) was also performed in order to evaluate cellular uptake, but with dosing of the IL-23 aptamer from an aqueous vehicle. Again the wash procedure removed aptamer from the skin surface (zero hour samples), confirming that fluorescence in the tissue results from topical penetration through the intact barrier (Figure 3). The IL-23 aptamer penetrated intact skin within 6 hours with fluorescence intensity increasing up to 24 hours. Fluorescence was detected in the extracellular matrix, as seen by the fluorescent gradient through the viable epidermis, and intracellular, confirmed by confocal imaging with fluorescence (potentially

within the nucleus) of keratinocytes in the *ex vivo* skin sections. This accords with anti IL-17A RNA aptamer uptake by cultured cells (Doble et al, 2014). Importantly, the distribution of the IL-23 aptamer suggests that topically delivered aptamers could modulate both intracellular and extracellular targets in the skin.

Detection and Quantitation of IL-23 aptamer in human skin

The fluorescence images suggest topical delivery of RNA aptamers through intact SC. As the current paradigm is that biomacromolecules cannot penetrate intact human skin, a dual hybridization assay (DHA) was developed where detection and capture probes quantified IL-23 aptamer extracted from the skin. The DHA selectivity and sensitivity was systematically verified through removal of nucleotides from both 5' and 3' ends of the aptamer and the capture/detection probes; single nucleotide removals resulted in loss of detection. Complete loss was observed when two or more nucleotides were removed at the expected skin concentration of <1,000 pM. The IL-23 aptamer was formulated into both cream and microemulsions, suggested as optimal vehicles for topical delivery of peptides and proteins (Russell-Jones and Himes, 2011), applied to freshly excised human skin mounted in flow through diffusion cells and removed at 0, 6 and 24 hours. The epidermis was removed by heat-separation (the temperature of which has been previously shown not to damage the aptamer) to allow extraction and quantification of the IL-23 aptamer in both the epidermis and dermis. Very low concentrations of IL-23 aptamer (0.09 – 0.36 μg) were in the epidermis and dermis after the initial (control) washing procedure (Figure 4a) but these levels were subtracted from the six and twenty four hour treated samples to account for any aptamer remaining after the wash procedure (Figure 4b).

Both vehicles delivered IL-23 aptamer to concentrations that exceeded by several orders of magnitude the desired cellular IC_{50} into both the epidermis and dermis, with delivery increasing in a time dependent fashion (Figure 4b). Interestingly, the cream delivered more aptamer compared to the microemulsion; 3.4 and 5.5 fold greater levels in the epidermis and dermis respectively following 6 hours of application ($P<0.009$ epidermis and $P<0.06$ dermis) with 1.5 (epidermis) and 2.3 fold (dermis) increases after 24 hours treatment ($P<0.06$ epidermis and $P<0.04$ dermis). The cream delivered 4 μg (14 μM, 4% of the applied aptamer dose) and 12 μg (37 μM, 12% of the applied dose) of IL-23 aptamer into the epidermis after 6 and 24 hour treatment respectively, which is approximately 43,000 and 119,000-fold above the cellular IC_{50} as shown in STAT3 activation of primary human T-cells (Figure 1e). The

cream delivered 0.6 μg (0.9 μM, 0.6% of the applied aptamer) and 0.7 μg (1.2 μM, 0.7% of the applied dose) to the dermis after 6 or 24 hours respectively, i.e. some 2,500 and 3,400 fold above the cellular IC_{50} for the IL-23 aptamer. In parallel, aptamer was also applied from an aqueous (control) solution at 10 mg/cm^2 but provided lower delivery; for example, 6 h post dose, 0.3 and 0.1 μg of the aptamer was detected in the epidermis and dermis respectively.

To demonstrate that the aptamer did not degrade during transit through the skin, an oligonucleotide precipitation assay using the DHA capture probes extracted the IL-23 aptamer from skin and was then visualized by polyacrylamide gel electrophoresis. The extracted RNA bands aligned with the IL-23 aptamer standards. Further, the relative band intensities correlated with the quantified values from the above DHA. Similar to the relative aptamer levels delivered by the two vehicles in the DHA, a more intense band was visualized for the cream compared to the microemulsion (Figure 4c and d).

Topical application of IL-23 aptamer inhibits Th17 derived cytokines in human skin

The above studies demonstrate that therapeutically relevant levels of aptamer can be delivered to, and recovered from, intact human epidermal and dermal tissue. An *ex vivo* human Th17 polarized skin model was used to further confirm delivery and intrinsic pharmacodynamics of this aptamer. Freshly excised human skin was mounted in static cells with growth media as the reservoir, and the skin was stimulated to induce a Th17 response (Smith, et al, 2016). The activity of the topically delivered IL-23 aptamer in the skin was compared to a basolateral treatment with IL-23 aptamer and an ROR gamma inverse agonist. The Th17 stimulating conditions significantly upregulated IL-17f, and 22 (Figure 5). Topical application of the IL-23 aptamer (1% aqueous solution of IL-23) decreased both IL-17f and IL-22 by approximately 45% ($p<0.001$ and 0.05 respectively) similar to those observed when IL-23 aptamer was included in the media (10μM IL-23). The addition of IL-23 aptamer, either topically or basolaterally, did not result in significant changes to IL-23 mRNA levels, confirming that the aptamer was not globally suppressing mRNA levels, but was specific for IL-17f and IL-22. Interestingly, the reduction of IL-22 mRNA following topical application of IL-23 aptamer was similar to that of the small molecule ROR gamma inverse agonist. These results confirm that skin penetrating aptamer retains the biologically active conformational structure capable of binding to endogenous IL-23.

DISCUSSION

In general, the literature does not support the ability of large molecules, particularly biomacromolecules, to significantly transit the stratum corneum passively to gain entry into the skin. Here, it is demonstrated that a 62-nucleotide (MW=20,395) mRfY aptamer not only transits the SC, but does so to therapeutically relevant levels in the epidermis and dermis. Multiple approaches demonstrate passage through the intact SC into the viable epidermis, including (i) fluorescently labelled aptamer (using two different labels) confirmed with gel electrophoresis, (ii) confocal microscopy, and (iii) dual hybridization assay using capture and detection probes with oligonucleotide precipitation. In contrast, topically administered domain antibodies failed to penetrate the SC or enter the viable epidermis. The aptamer within skin far exceeded the desired cellular IC_{50} values (119,000-fold > IC_{50} in the epidermis; 3,400-fold > IC_{50} in the dermis) following 24 h delivery from a simple cream formulation. Additionally, intracellular and extracellular localization was observed. Nonspecific uptake of an RNA aptamer into primary human keratinocytes has been previously reported (Doble et al, 2014), though the authors noted that site-specific (i.e., topical) treatment to reduce inflammatory mediators produced by deeper keratinocytes would be problematic due to aptamer uptake by upper skin layer keratinocytes. In our studies, topically delivered IL23 aptamer suppressed IL-17 and IL-22 mRNA production in a cytokine stimulated *ex vivo* human skin model, showing that the aptamer is available to exert a therapeutic effect in deeper skin layers confirming the fluorescence, dual hybridization assay, and oligonucleotide precipitation assay data.

There are conflicting reports on the feasibility of topical delivery of antisense oligonucleotides, though notably none are clinically approved (Butler et al, 1997; Mehta et al, 2000; White et al, 1999; White et al, 2002). Aptamers are a class of oligonucleotide-based technologies that can bind to a wide range of molecules and have been mainly used for diagnostics and systemic therapeutics. In contrast to antisense oligonucleotides, aptamers offer significant conformational plasticity and flexibility (Nomura et al, 2010). The structure and composition of aptamers can be modified but retain significant activity, whereas modifications to antisense molecules are avoided because of their potential impact on efficacy. The literature reports rapid systemic clearance of aptamers, limiting unwanted side effects and restricting the biologic effects of topically administered aptamers to the skin

(Healy et al, 2004; Watson et al, 2000). Thus, RNA aptamers represent a broad class of biological compounds that could be used for local targeting of skin diseases.

Since our results contradict the "normal" rules governing molecular properties and topical drug delivery, numerous potential mechanisms by which the aptamer enters the tissue were explored (and will be described in detail in a further publication). However, the role of water was probed by hydrating the stratum corneum for 12 h prior to dosing and by occluding (or not) the both pre-hydrated and none pre-hydrated tissue, using finite (5-10 mg/cm^2) and infinite (300 mg/cm^2) doses of the aptamer in an aqueous vehicle alongside blank controls for detection at 6 and 15 h in the epidermis and dermis, as above. In short, the water gradient across skin was removed by fully hydrating or occluding the stratum corneum; pre-hydrating the tissue was broadly detrimental but occlusion was generally beneficial, most notably for infinite dosing of none pre-hydrated skin. Delivery of this highly water soluble aptamer thus appears to be influenced by changing the water gradients across the skin.

Since the conformational structure of aptamers can be disrupted by metal ions (notably Ca^{2+} and Mg^{2+}) that are present in human skin, aptamer delivery from aqueous vehicles was compared to delivery when the vehicle included 100 or 10 mM EDTA, or when 10 mM $CaCl_2$ or 10 mM $MgCl_2$ was added; similar studies also used these adjuncts in the receiving fluid. Neither chelating the ions with EDTA nor adding additional ions significantly impacted aptamer amounts in either the dermis or epidermis at 6 or 15 h post dosing.

Though active transport mechanisms are widely regarded as absent in the stratum corneum, it is feasible that some carrier systems may operate in the deeper skin layers. This was explored by comparing aptamer delivery at 4 and 32°C; amounts in the dermis and epidermis at 6 and 15 h post dosing were invariant with temperature confirming passive rather than active transport.

The optimised IL-23 aptamer is folded and the role of the secondary structure in its skin penetration was explored through comparison with a series of four variants containing secondary or tertiary modifications. 24 hour post dosing, all variants were detected in the epidermis; approximately 10% of the applied dose of the optimised aptamer was detected whereas 17 – 5% of the variants doses were detected in this layer. Different IL-23 aptamers

with a range of molecular weights (from an 85-mer, mw = 28,950 Da to a 39-mer, mw = 13,435) were applied alongside a second series of aptamers against the transferrin receptor (85-mer, mw = 29,348; 45-mer, mw = 15,512; 36-mer, mw = 12,486). Fluorescence imaging showed that all the RNA-based aptamers penetrated into intact human skin and were visualised within the epidermis. In contrast to small "conventional" drugs, no molecular weight dependence on uptake was seen for the aptamers and, as a class, they appear to be able to penetrate the stratum corneum.

In summary, numerous mechanisms for aptamer uptake into intact human have been explored. From the fluorescence images, there is no evidence to suggest that delivery is principally via the shunt routes. For the large RNA-based structures, uptake is independent of molecular weight (between 12.5 and 29.3 kDA) and was unaffected by our secondary and tertiary conformational modifications. There is no evidence for active transport and divalent cation effects were not detected. Some delivery-dependence on tissue water content is seen, perhaps not surprisingly considering that these molecules are highly water soluble, but pre-hydrating the skin was detrimental whereas occlusion was generally beneficial.

This study demonstrates that, despite being very large molecular weight biotherapeutic agents, RNA aptamers can permeate across the intact human skin barrier to therapeutically relevant levels in both the epidermis and dermis.

MATERIALS AND METHODS

IL-23 Aptamer

Following in vitro selection (Supplementary Information S2), the IL-23 aptamer was fully minimized and optimised from 84 to 61 nucleotides using computational folding prediction programs and systematic deletion. Modifications at the 2' position of the sugar for each base were evaluated to improve activity as well as predicted in vitro stability either by substitution of a 2'Fluoro with a 2′-O-methoxyethyl(2'OME) (2'F -> 2'OMe) or substitution of a 2′-O-methoxyethyl with a 2'Fluoro (2'OMe->2'F). All tolerated or potency increasing substitutions were combined with all tolerated deletions within the oligonucleotide. Appendage of a 3'-inverted thymidine residue, to increase nuclease resistance, resulted in a 62 nucleotide long molecule (IL-23 aptamer) composed of ten 2'-O-methyladenosines (mA), one 2'-fluoroadenosine (fA), fourteen 2'-Omethylguanosines (mG), six 2'-fluoroguanosines

(fG), three 2'-O-methylcytosines (mC), thirteen 2'-fluorocytosines (fC), one 2'-O-methyluridine (mU), thirteen 2'-fluorouridines (fU) and the 3'-terminus is capped with a single inverted deoxythymidine residue to protect against nuclease degradation (MW= 20,395). The IL-23 RNA mRfY aptamer was conjugated with dylight 488 or Cy3 fluorescent labels as an amide conjugate during chemical synthesis.

Preparation of Human *Ex Vivo* Skin

Full-thickness human skin was obtained within several hours from patients undergoing elective abdominoplasty. The acquisition, written informed consent form (IFC), and protocol for use were approved by an independent Investigational Review Board (Pearl IRB, Indianapolis, IN). Immediately after collection, the skin was transferred to phosphate buffered saline (PBS) and kept at 4°C during transit. Subcutaneous fat was removed from the samples and the skin rinsed briefly in Hank's balanced salt solution with 1% antibiotic/antimycotic. Split-thickness dermatomed skin was prepared by placing full thickness skin on high-density foam blocks and cut to specified thickness (250 ± 100 µm, 500 ± 100 µm, or 750 ± 100 µm) using an Electro-Dermatome.

Skin was left untreated for uncompromised barrier (intact), pre-treated with sodium bicarbonate crystals to partially disrupt the barrier (abraded), or pre-treated with approximately 28 tape strips to completely remove the barrier (tape stripped). To confirm SC disruption, skin sections immediately after treatments were fixed in formalin and paraffin-embedded, sectioned and stained with H&E.

In Vitro Skin Penetration

Two different flow-through diffusion cells (PermeGear, Inc and Eclectech, Inc.) or static diffusion cells (PermeGear, Inc) were used to assess aptamer permeation and activity.

Flow through diffusion system: Flow-through diffusion cells were placed in cell warming supports to maintain the skin surface temperature at 32 ± 2°C. Cells were connected to multi-channel peristaltic pumps via Tygon® tubing, and the cell outlets were fitted with poly ether ether ketone (PEEK) tubing, angled to drip into 96-well plates or 20 mL vials on fraction collectors. Dermatomed *ex vivo* human skin was mounted in the diffusion cells, SC side up. Donor compartment blocks placed on the skin were secured to provide a leak proof seal, exposing a surface area of 1.0 cm^2. The pumps were adjusted to maintain sink conditions with a flow-rate of 0.300 mL/hour (5.0 µL/minute) or 3.6 mL/hour (60 µL/minute) for the

ChanneL cells and PermeGear Cells respectively with phosphate buffered saline used as the receiving fluid. Both systems were allowed to equilibrate for ~30 min prior to dosing.

Static diffusion cell system: Static (Franz-type) cells were used for the Th17 stimulated human ex-vivo skin model. Briefly, dermatomed *ex vivo* skin was mounted SC side up on static diffusion cells with an average surface area of approximately 0.6 cm² and a receiver compartment volume of approximately 2.0 mL. The receiver chamber was initially filled with cornification media and incubated at 37°C. Then skin was dosed topically or systemically (in the media) with aptamer for twenty-four hours before the receiver solution was replaced with Th17 stimulation cocktail. Twenty-four hours after stimulation, the tissue was harvested, minced before RNA isolation and quantitation. Full details can be found in Supplementary Information S4.

Dosing and vehicles: The IL-23 aptamer was formulated at 1% in either an oil-in-water cream (62.5% Di water, 0.5% Benecel MP333C, 10% Isopropyl Myristate, 10% Glyceryl Monostearate NSE 400, 15% Polyoxyl-40-stearate, and 1% Phenonip), microemulsion (5% Isopropanol, 20% Di water, 1.5% benzyl alcohol, 30% Drakeol-5, 15% Brij 02, 15% Brij 010, 12.5% cetrimonium chloride) or water vehicle (controls; 98.9% DI Water, 0.1% Polysorbate 20, 1% Benzoyl alcohol). The formulations were uniformly dosed onto the SC surface using a positive displacement pipette, set to deliver 10 mg/cm^2. The donor chambers were left open to ambient conditions, i.e., the skin was not occluded.

Post-dosing skin washing and isolation: At predetermined time points (0, 4, 6, 15, or 24 hours), the skin was thoroughly cleansed. Three cotton buds; dry, wet (1:9 Hexane:MeOH or 0.05% Tween 20 in PBS) and dry were used to remove the surface formulation and was immediately followed by 3 consecutive tape strips (Scotch® Transparent Tape 175L-WG). These samples were not analysed and considered as surface deposited compound, i.e. not penetrating the skin. Heat separation of skin layers by soaking in hot water was avoided to prevent migration of aptamer or biomarkers. Thus, post treatment, the skin was placed in an oven at 60°C for 2 minutes, and the epidermis was carefully separated from the dermis using forceps. Epidermis and dermis samples analysed by the dual hybridization assay (DHA) were placed into separate vials and 1 mL of 0.25 % trypsin was added to each. Vials were placed in an oven set at 37°C for 16 to 20 hours and then the extraction diluent was removed and centrifuged at 13,000 RPM for 10 minutes to remove residual materials.

Conjugated Fluorescence Detection

Dried skin (cleaned as above) was placed epidermis side down on a clean cutting board and smaller sections cut with a clean razor blade to avoid carry over. Sections were placed on edge in 15x15 mm moulds and immediately frozen in OCT using an isopentane/dry ice bath. Moulds were then wrapped in aluminium foil, and stored at -80°C. For immunofluorescence (IFC), the frozen blocks were placed into a -20°C cryostat 3 minutes prior to sectioning. Five µm sections were cut and mounted on individual Richard Allen Bond-Rite slides which were fixed in -20˚C acetone for 10 minutes and then air dried for 30 minutes. Slides were rinsed three times with Tris Buffered Saline (TBS) (Dako). Slides with nuclear staining were cover-slipped with ProLong® Gold Antifade Reagent with diamidino-2-phenylindole (DAPI) (Invitrogen). Permeation was assessed using a fluorescence microscope fitted with appropriate filters for the fluorophore. Images were taken using a Leica DMRXA2 microscope mounted with a Nikon DS-QiMc monochromatic camera and NIS Elements BR 3.2 software. For each independent experiment, skin was also dosed with vehicle alone (control) and all pictures were taken using the same exposure time to discard auto-fluorescence signals from skin or fluorescence from residual vehicles.

Dual Hybridization Assay

The dual hybridization assay (DHA) has been previously used with plasma and vitreous humour samples (Drolet et al, 2000). This assay is analogous to an ELISA where aptamer is allowed to hybridize to capture and detection DNA oligonucleotide probes. The capture probe (ARC35141; Integrated DNA Technologies) binds to the 13 nucleotides at the 5'-terminus of the aptamer and was covalently attached to magnetic beads via a 3'-terminal amino linker. The detection probe (ARC35156; Integrated DNA Technologies) was complementary to the 15 nucleotides at the 3'-terminus of the aptamer and was biotinylated at the 5'-terminus. Further details are available in the accompanying Supplementary Information (S3)

The recovered aptamer (mass per cm^2) from each skin layer was converted to concentration (µmol/L) where the volume of epidermis was assumed to be 0.015 cm^3 and the volume of dermis was assumed to be 0.035 cm^3.

Oligo-Protein Precipitation Assay

To confirm aptamer quantitation by DHA, an assay was developed, termed oligo-precipitation "OP". This used the same biotinylated capture primers from the DHA to mix with the 100 μL of digested skin samples (epidermis or dermis). Samples were heated and cooled to allow primer to hybridize. Streptavidin beads were added to pull down the aptamer-primer complex. The aptamer was then eluted off the beads, loaded onto a 15% urea gel and stained with Sybr Gold to visualize and compare aptamer bands.

Th17 Stimulated Human *Ex Vivo* Skin Model

Th17-skewed cytokine expression was induced from *ex vivo* skin-resident immune cells according to our earlier report demonstrating efficacy of a RORγ inverse agonist small molecule (Smith et al, 2016). Details can be found in Supplementary Information (S4).

CONFLICT OF INTEREST

At the time of the study, Jon Lenn, Jessica Neil, Christine Donahue, Kellie Demock, Caitlin Vestal Tibbetts, Susan H. Smith, David Rubenstein and Jean-Philippe Therrien were employees of GlaxoSmithKline; Javier Cote-Sierra was employed by Pfizer; P. Shannon Pendergrast was employed by Ymir Genomics; Jason Killough was employed by Momenta Pharmaceuticals; Marc Brown was employed by MedPharm.

ACKNOWLEDGEMENTS:

Madaline Gilbert for work on the endogenous IL-23 production. Kofi Nyam, Ayesha Paul, and Bhasha Desai worked on the skin penetration studies. Michael Luke, Mary Larm, Leon Loupenok developed the IL-23 cream and microemulsion formulations. Charlotte Stewart, Rob Turner, and Jennifer Nelson for help with the DHA analysis. Robert Hale, Christopher Arico-Muendel for their help with labelled aptamers. Beth Millerman for histological sections. Thi Bui, and Kathleen Richter for their help with the development of the target engagement *ex vivo* skin model.

REFERENCES

Blauvelt A. T-helper 17 cells in psoriatic plaques and additional genetic links between IL-23 and psoriasis. J Invest Dermatol 2008; 128:1064-1067.

Bos JD, Meinardi MM. The 500 Dalton rule for the skin penetration of chemical compounds and drugs. Exp Dermatol 2000; 9:165-169.

Butler M, Stecker K, Bennett CF. Cellular distribution of phosphorothioate oligodeoxynucleotides in normal rodent tissues. Lab Invest 1997; 77:379-388.

Darisipudi MN, Kulkarni OP, Sayyed SG, Ryu M, Migliorini A, Sagrinati C et al. Dual blockade of the homeostatic chemokine CXCL12 and the proinflammatory chemokine CCL2 has additive protective effects on diabetic kidney disease. Am J Pathol 2011; 179:116-124.

Di Cesare A, Di Meglio P, Nestle FO. The IL-23/Th17 axis in the immunopathogenesis of psoriasis. J Invest Dermatol 2009; 129:1339-1350.

Doble R, McDermott MF, Cesur O, Stonehouse NJ, Wittmann M. IL-17A RNA aptamer: possible therapeutic potential in some cells, more than we bargained for in others? J Invest Dermatol 2014; 134:852-855.

Drolet DW, Nelson J, Tucker CE, Zack PM, Nixon K, Bolin R, et al. Pharmacokinetics and safety of an anti-vascular endothelial growth factor aptamer (NX1838) following injection into the vitreous humor of rhesus monkeys. Pharm Res 2000; 17:1503-1510.

Healy JM, Lewis SD, Kurz M, Boomer RM, Thompson KM, Wilson C, et al. Pharmacokinetics and biodistribution of novel aptamer compositions. Pharm Res 2004; 21:2234-2246.

Keefe AD, Pai S, Ellington A. Aptamers as therapeutics. Nat Rev Drug Discov 2010; 9:537-550.

Koutruba N, Emer J, Lebwohl M. (2010) Review of ustekinumab, an interleukin-12 and interleukin-23 inhibitor used for the treatment of plaque psoriasis. Ther Clin Risk Manag 2010; 6:123-141.

Mehta RC, Stecker KK, Cooper SR, Templin MV, Tsai YJ, Condon TP, et al. Intercellular adhesion molecule-1 suppression in skin by topical delivery of anti-sense oligonucleotides. J Invest Dermatol 2000; 115(5):805-812.

Ng EW, Shima DT, Calias P, Cunningham ET Jr, Guyer DR, Adamis AP. Pegaptanib, a targeted anti-VEGF aptamer for ocular vascular disease. Nat Rev Drug Discov 2006; 5:123-132.

Nomura Y, Sugiyama S, Sakamoto T, Miyakawa S, Adachi H, Takano K, et al. Conformational plasticity of RNA for target recognition as revealed by the 2.15 A crystal structure of a human IgG-aptamer complex. Nucleic Acids Res 2010; 38:7822-7829.

Parunov LA, Fadeeva OA, Balandina AN, Soshitova NP, Kopylov KG, Kumskova MA, et al. Improvement of spatial fibrin formation by the anti-TFPI aptamer BAX499: changing clot size by targeting extrinsic pathway initiation. J Thromb Haemost 2011; 9:1825-1834.

Russell-Jones G, Himes R. Water-in-oil microemulsions for effective transdermal delivery of proteins. Expert Opin Drug Deliv 2011; 8:537-546.

Schwoebel F, van Eijk LT, Zboralski D, Sell S, Buchner K, Maasch C et al. The effects of the anti-hepcidin Spiegelmer NOX-H94 on inflammation-induced anemia in cynomolgus monkeys. Blood 2013; 121:2311-2315.

Smith S, Carlos E, Peredo CE, Yukimasa Takeda Y, Bui T, Neil J, Rickard D et al. Development of a Topical Treatment for Psoriasis Targeting RORγ: From Bench to Skin. PLOS ONE, doi: 10.1371/journal.pone.0147979.

Sofen H, Smith S, Matheson RT, Leonardi CL, Calderon C, Brodmerkel C et al. Guselkumab (an IL-23-specific mAb) demonstrates clinical and molecular response in patients with moderate-to-severe psoriasis. J Allergy Clin Immunol 2014; 133:1032-1040.

Tausend W, Downing C, Tyring S. Systematic review of interleukin-12, interleukin-17, and interleukin-23 pathway inhibitors for the treatment of moderate-to-severe chronic plaque psoriasis: ustekinumab, briakinumab, tildrakizumab, guselkumab, secukinumab, ixekizumab, and brodalumab. J Cutan Med Surg 2014; 18:156-169.

Watson SR, Chang YF, O'Connell D, Weigand L, Ringquist S, Parma DH. Anti-L-selectin aptamers: binding characteristics, pharmacokinetic parameters, and activity against an intravascular target in vivo. Antisense Nucleic Acid Drug Dev 2000; 10:63-75.

White PJ, Fogarty RD, Liepe IJ, Delaney PM, Werther GA, Wraight CJ. Live confocal microscopy of oligonucleotide uptake by keratinocytes in human skin grafts on nude mice. J Invest Dermatol 1999; 112:887-892.

White PJ, Gray AC, Fogarty RD, Sinclair RD, Thumiger SP, Werther GA, et al. C-5 propyne-modified oligonucleotides penetrate the epidermis in psoriatic and not normal human skin after topical application. J Invest Dermatol 2002; 118:1003-1007.

Williams AC. Transdermal and Topical Drug Delivery: from Theory to Clinical Practice, Pharmaceutical Press, London, UK 2003; 242.

Wingens M, Pfundt R, van Vlijmen-Willems IM, van Hooijdonk CA, van Erp PE, Schalkwijk J. Sequence-specific inhibition of gene expression in intact human skin by epicutaneous application of chimeric antisense oligodeoxynucleotides. Lab Invest 1999; 79:1415-1424.

FIGURE LEGENDS

Figure 1. Predicted secondary structure of the fully minimised and optimized IL-23 aptamer using mfold.

Figure 2. Penetration of IL-23 aptamer through compromised and uncompromised human skin. (a). Penetration of IL-23 dylight 488 labelled aptamer (green) into intact, abraded and tape stripped human abdominal skin showing aptamer distribution after washing from the skin surface immediately after dosing (wash control) and 4 hours post dosing. (b) Distribution of a single domain fully human antibody (dAb) fragment (13.1 kDa) dosed topically onto tape stripped skin. (c) Polyacrylamide gel of fluorescent aptamer extracted from intact (untreated, UNT) and abraded (Abr) skin compared to IL-23 aptamer dylight 488 standard (IL-23 Aptamer) and a 28-mer SDF-1 aptamer (28-mer).

Figure 3. Topically applied IL-23 aptamer penetrates human skin and into keratinocytes. (a) Penetration of IL-23 Cy3 labelled aptamer (orange) into intact human abdominal skin after zero (wash control), 6 and 24 hours post dosing. (b). Uptake of IL-23 aptamer into skin keratinocytes (dashed lines indicating the epidermal junction). (c) Intracellular uptake of aptamer (green) with nuclear DAPI stain (blue) used for cellular orientation.

Figure 4. Dual Hybridization Assay (DHA) and Oligonucleotide Precipitation to quantify intact aptamer within skin. (a) Aptamer recovery by DHA from epidermis following zero (wash control), 6 and 24 hours application from a microemulsion and cream formulation. (b) Aptamer recovery by DHA from dermis following zero (wash control), 6 and 24 hours application from a microemulsion and cream formulation. (c) Polyacrylamide gel of aptamer extracted from the epidermis by oligonucleotide precipitation following dosing from a cream (Crm) compared to the IL-23 aptamer standard (Std=80 ng). (d) Polyacrylamide gel of aptamer extracted from the dermis by oligonucleotide precipitation following dosing from a cream (Crm) and microemulsion (ME) compared to IL-23 aptamer standards (40ng, 20ng, 10ng, 5ng, 2.5ng, 1.25ng, 0.6ng). DHA data shown as mean ± SEM, n=5.

Figure 5. Topical application of IL-23 aptamer inhibits Th17 derived cytokines in human skin. Freshly excised human abdominal skin was mounted and clamped in place using static cells containing growth media and stimulated twenty four hours later to induce a Th17 response. The skin was treated topically twice with 8 µL of IL-23 aptamer (210 µg/cm2) in an aqueous vehicle before and concurrent with Th17 stimulation. IL-23 aptamer (10 µM) and a RORgamma inverse agonist (10 µM; small molecule) was included in the media as systemic controls. Twenty-four hours post stimulation, skin was harvested and relative transcript levels of Th17-type cytokines, IL-17f (a), IL-22 (b), and IL-23 (c) were determined by qPCR. Bars represent the mean percent of maximum stimulation (set to 100%) from 3 different skin donors (n=3).

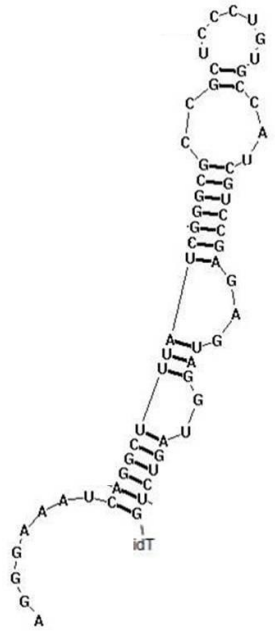
idT

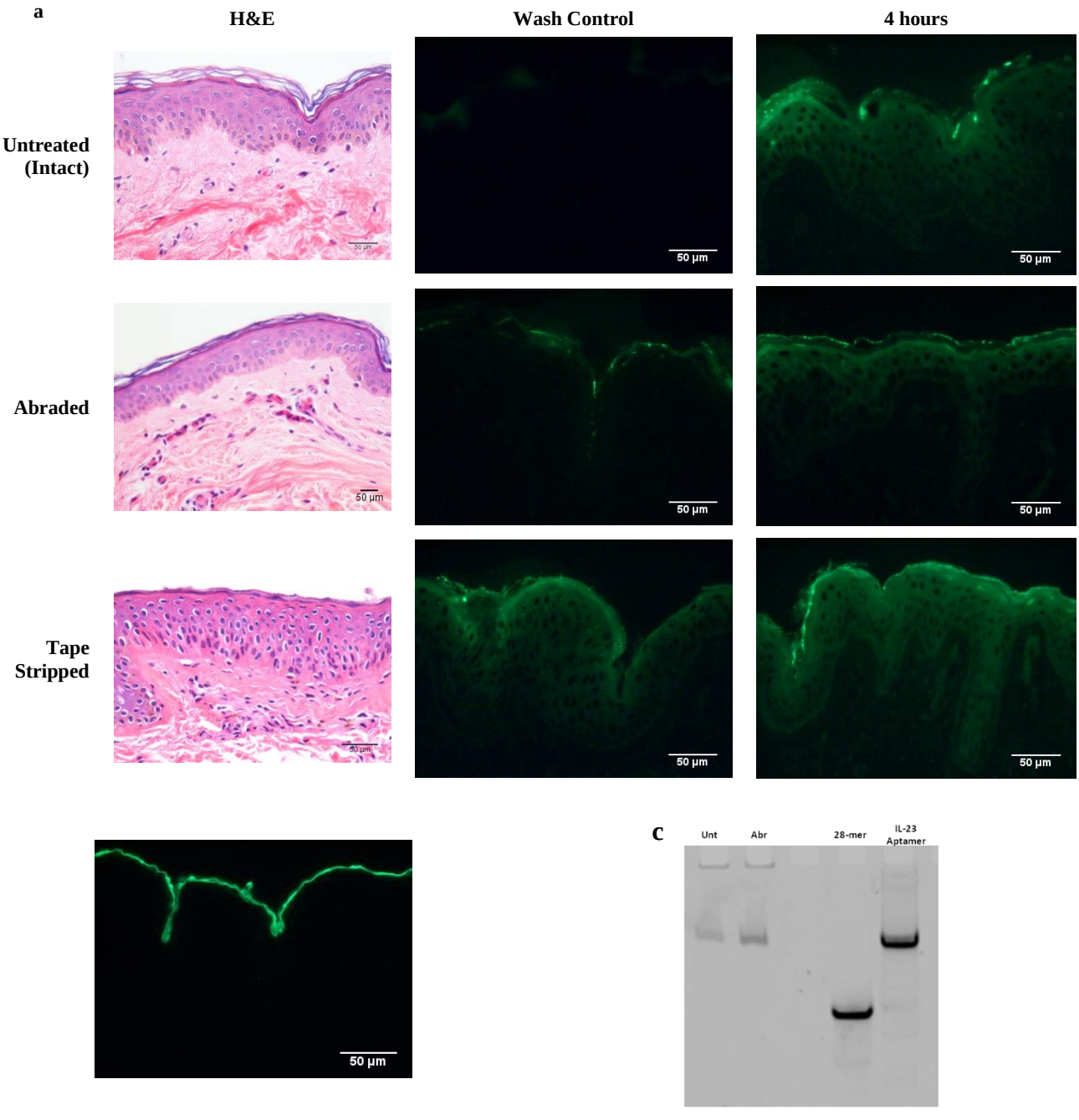
a
H&E
Wash Control
4 hours
Untreated (Intact)
Abraded
Tape Stripped
50 µm
b
50 µm
c
Unt
Abr
28-mer
IL-23 Aptamer

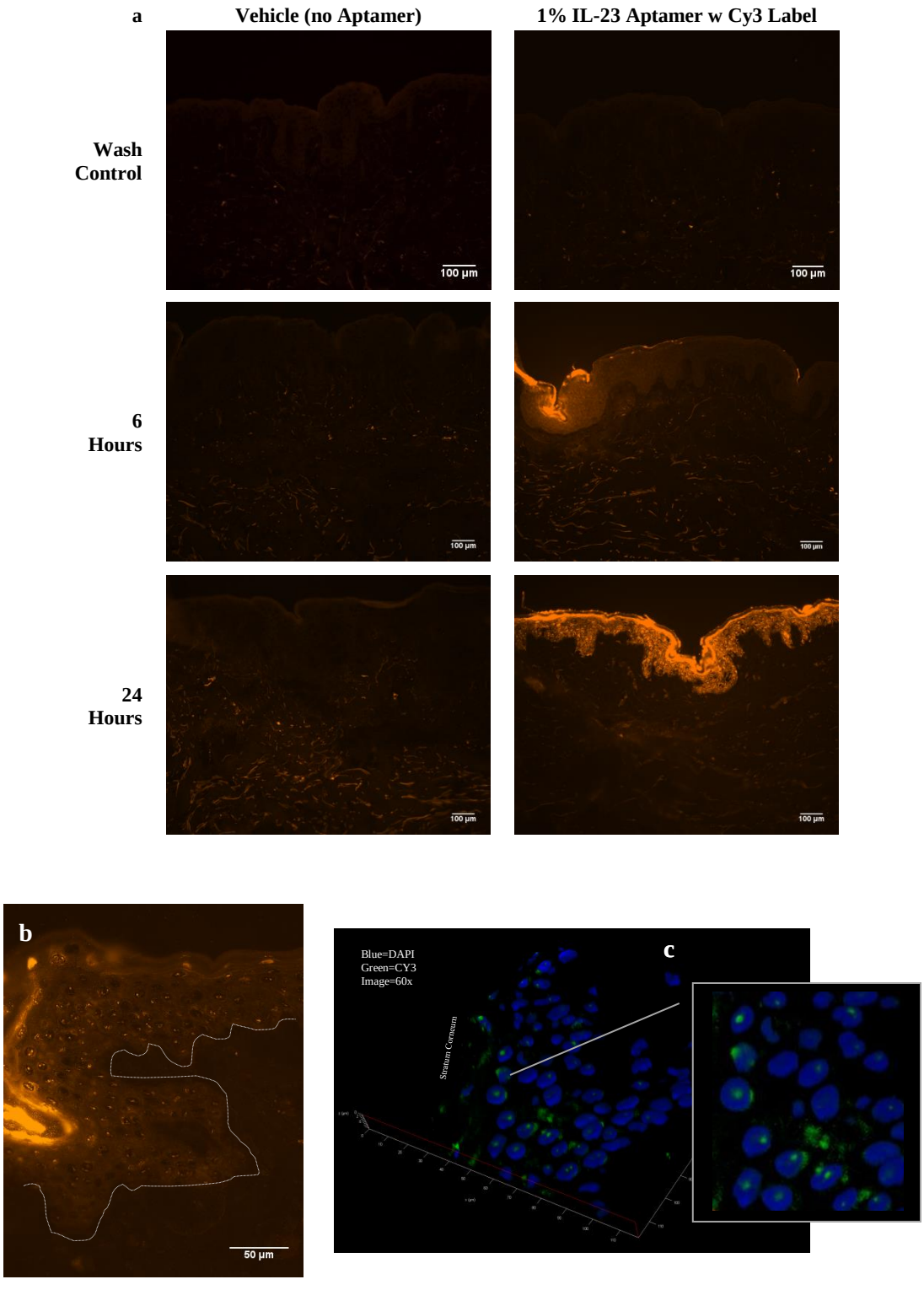
a
Vehicle (no Aptamer)
1% IL-23 Aptamer w Cy3 Label
Wash Control
6 Hours
24 Hours
100 µm
b
50 µm
c
Blue=DAPI
Green=CY3
Image=60x
Stratum Corneum

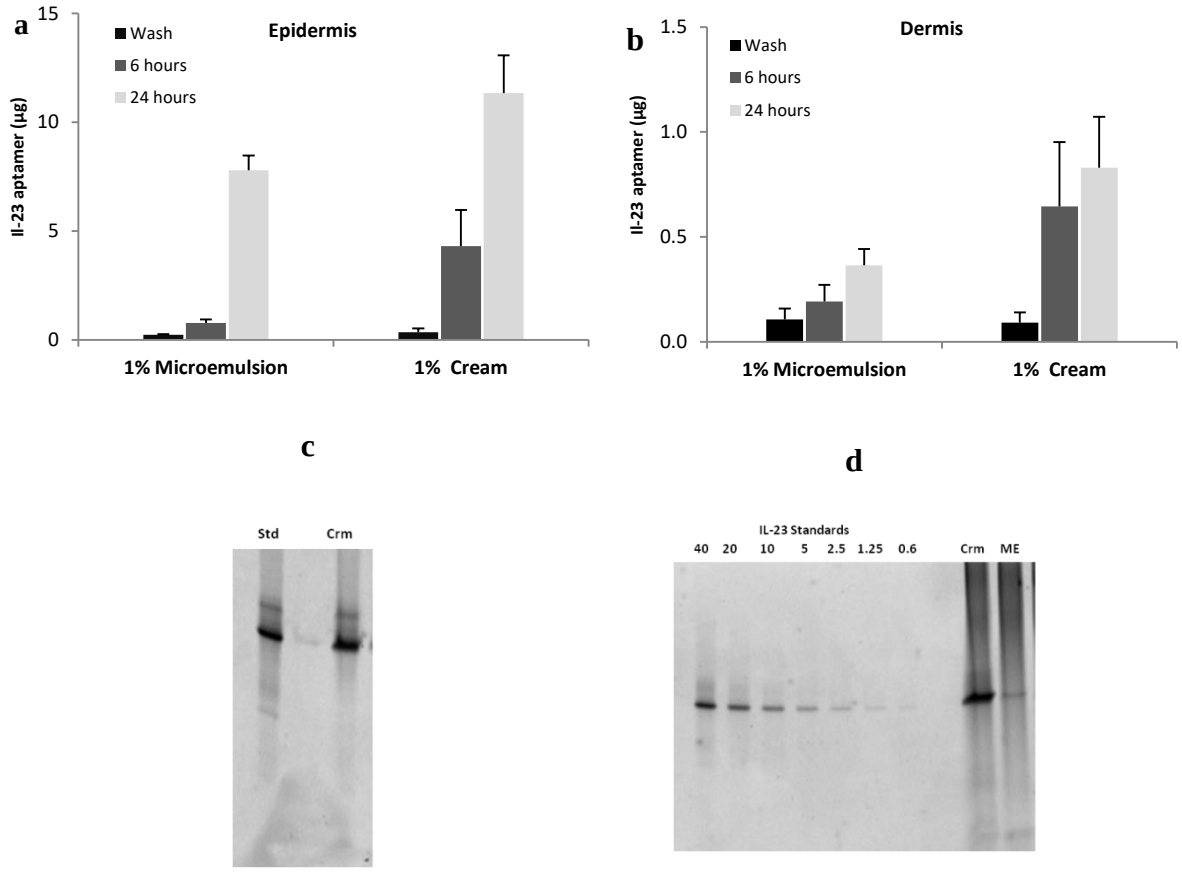
a
Epidermis
Wash
6 hours
24 hours
Il-23 aptamer (µg)
15
10
5
0
1% Microemulsion
1% Cream
b
Dermis
Wash
6 hours
24 hours
Il-23 aptamer (µg)
1.5
1.0
0.5
0.0
1% Microemulsion
1% Cream
c
Std
Crm
d
IL-23 Standards
40 20 10 5 2.5 1.25 0.6
Crm ME

Figure 5

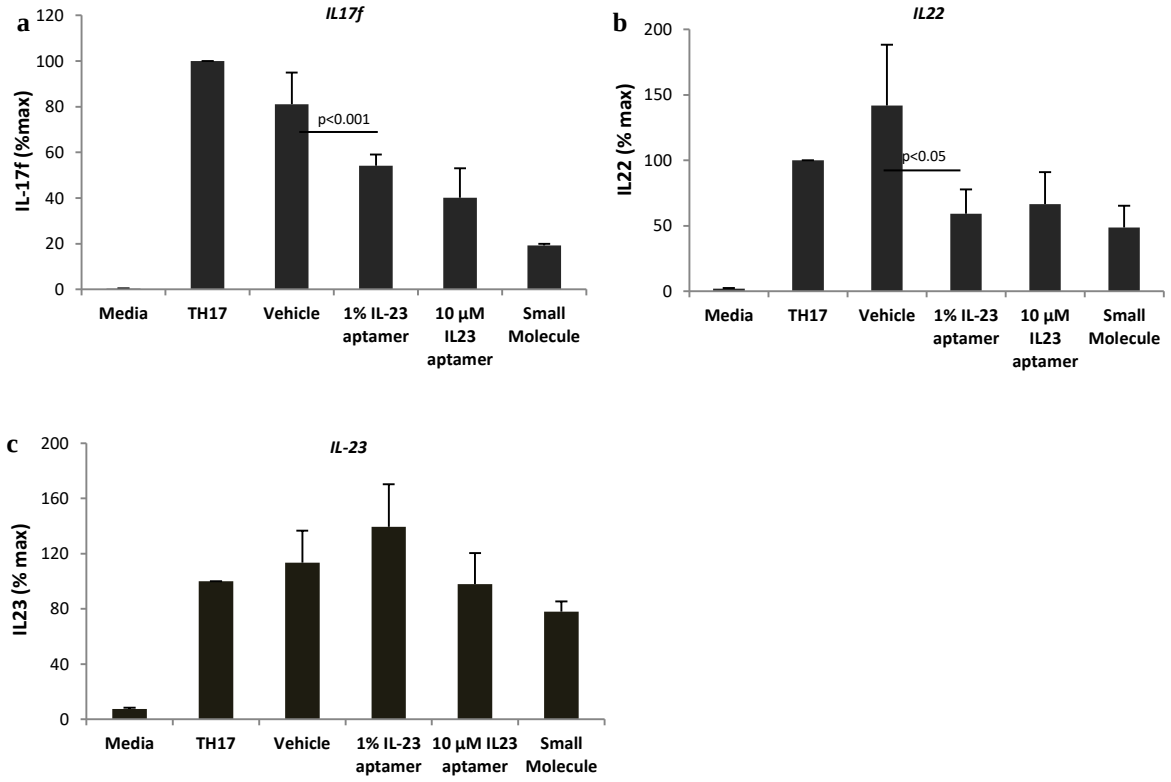
a
IL17f
IL-17f (%max)
120
100
80
60
40
20
0
p<0.001
Media
TH17
Vehicle
1% IL-23 aptamer
10 µM IL23 aptamer
Small Molecule
b
IL22
IL22 (% max)
200
150
100
50
0
p<0.05
Media
TH17
Vehicle
1% IL-23 aptamer
10 µM IL23 aptamer
Small Molecule
c
IL-23
IL23 (% max)
200
160
120
80
40
0
Media
TH17
Vehicle
1% IL-23 aptamer
10 µM IL23 aptamer
Small Molecule

Supplementary Information. S1

The IL-23 aptamer is biologically active

STAT3 Activity in PHA-Blast cells

Endogenous IL-23 was prepared from the conditioned media of activated purified primary human monocytes by affinity purification. Peripheral Blood Mononuclear Cells (PBMC) were obtained from buffy coats prepared from fresh human blood. Monocytes were isolated by adherence to CD14 coated magnetic beads (Miltenyi, Cologne, Germany). To induce and enhance IL-23 expression, monocytes were treated with LPS and anti-IL-10 blocking antibodies. After 24 hours, conditioned media was collected and frozen. Sepharose NHS agarose beads (Sigma, St. Louis, MI) were coupled with non-neutralizing p19 monoclonal antibodies (eBioscience, San Diego, CA) and incubated overnight with pooled conditioned media from multiple donors. Beads were washed and endogenous IL-23 eluted with acid, and neutralized with a TRIS-base, BSA containing buffer. The eluate was dialyzed with PBS, and the purified protein was aliquoted and frozen. Expression of IL-23 from monocytes was confirmed by testing conditioned media using the p19/p40 enzyme-linked immunosorbent assay (ELISA) from eBioscience (San Diego, CA). The ELISA plate was coated with an anti-p19 antibody and captured antigen was detected with an anti-p40 antibody, thus specifically measuring the IL-23 cytokine. A titration of purified protein was applied to IL-2/PHA activated T-cells for 15 minutes to induce the phosphorylation of STAT3. pSTAT3 (phospho-STAT3) in cell lysates were subsequently measured by ELISA (Cell Signalling Technologies, Danvers, MA). Phosphorylated STAT3 from PHA Blast cells treated with purified endogenous IL-23 was measured by colorimetric ELISA after 15 minutes of stimulation with dialyzed eluate. The endogenous protein was subsequently used in PHA Blast phospho-STAT3 assays at a volume falling in the linear range of the curve. Titration curves were generated using PHA blasts from seven different donors and tested at concentrations between 0.00057 and 500 nM. Seven 12-point titration curves, each in duplicate, were used to calculate a mean (+/- SEM).

Phospho-STAT3 assay

IL-23 aptamer inhibition of endogenous IL-23 activation of PHA/IL-2 activated T- cells was tested by measuring levels of phospho-STAT3. Binding of IL-23 to its receptor on activated T-cells stimulates several STAT pathways, including STAT3. PBMC's from fresh human blood (Archemix) were isolated by centrifugation in a histopaque gradient and treated with PHA/IL-2 to enrich for T-cells and to upregulate IL-23 receptors. Cells were serum starved and treated with endogenous IL-23 for 15 minutes, then lysed. Relative levels of phospho-STAT3 in IL-23 treated lysates, in the presence and absence of IL-23 aptamer or a neutralizing p19 antibody, were measured by ELISA (Cell Signalling Technologies, Danvers, MA). Titrations of aptamer/antibody were used to generate inhibition curves from which the cellular IC50 determinations were made.

Results

Three different cellular assays demonstrated biological activity of the aptamer. (I) Inhibition of IL-23 dependent stimulation of STAT3 activity in PHA-Blast cells showed that both the parent full length IL-23 aptamer (84-mer) and minimer (61-mer) were biologically active (Figure 1a). The parent cellular IC50 was 0.26 nM ± 0.036 nM and the more potent minimized aptamer IC50 was 0.075 nM ± 0.030 nM (Figure 1b). The activity of both aptamers was greater than the control anti-p19 antibody, cellular IC50=0.69 nM ± 0.12 nM. (II) Receptor binding of IL-23 on activated T-cells stimulates several STAT pathways, including STAT3. The ability to block endogenous IL-23 activation in PHA/IL-2 activated T-cells, evaluated by measuring levels of phospho-STAT3, also demonstrated aptamer biological activity; representative anti-p40 antibody and IL-23 aptamer inhibition curves are in Figure 1b. (III) Finally, the ability of the IL-23 aptamer to inhibit IL-12 activation of PHA/IL-2 activated T-cells was evaluated. Similar to IL-23, IL-12 receptor binding on activated T-cells stimulates several STAT pathways, including STAT3 and many IL-23 antagonists also inhibit IL-12 since they share the p40 subunit. The IL-23 aptamer only inhibits IL-23 activation and not IL-12 activation, much like the anti-p19 antibody. Representative p19 antibody and IL-23 aptamer inhibition curves (Figure 1c) show that the IL-23 aptamer is specific for IL-23. From seven 12-point titration curves, each in duplicate, the mean (±SEM) cellular IC50 was 296 ± 90 pM for the IL-23 aptamer (Figure 1d). The IL-23 aptamer has > 500 nM binding affinity to IL-12 as assessed by a radiolabelled dot blot assay.

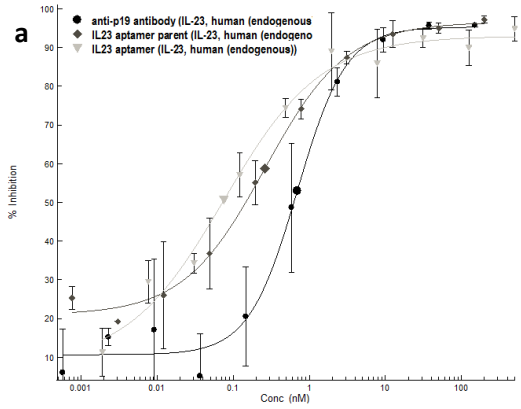

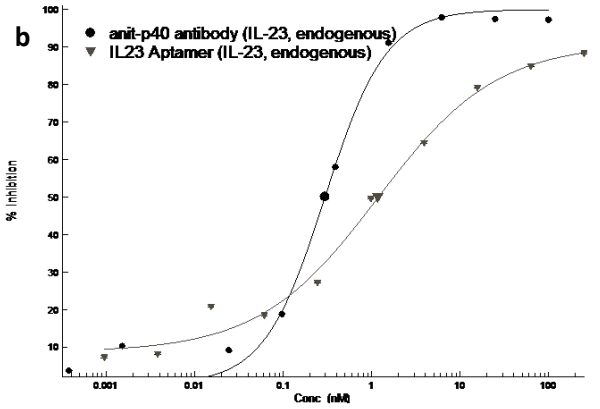

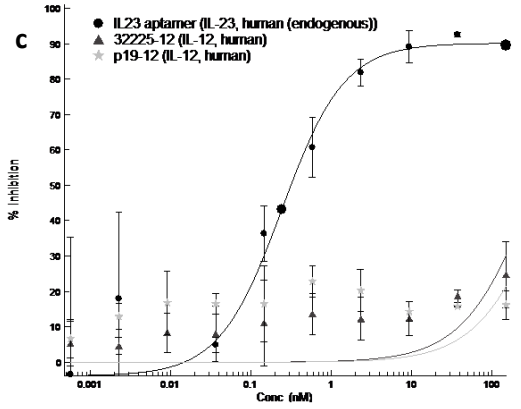

d

IC_{50} (nM)		
Donor	p19	IL-23 Aptamer
1	2.84	0.714
2	8.82	0.075
3	0.088	0.033
4	0.172	0.243
5	0.896	0.271
6	0.426	0.241
7	1.04	0.501
Mean	**2.04**	**0.296**
SEM	1.18	0.09

Figure S1. The selection and cellular activity of the IL-23 aptamer. (a) Functional activity following minimization and optimization of the IL-23 aptamer. (b) IL-23 aptamer inhibition of endogenous IL-23 in the PHA Blast phospho-STAT3 assay. (c) Activity of the IL-23 aptamer against eIL-23 and rIL-12. (d) Percent inhibition by p19 neutralizing antibody and the IL-23 aptamer in the PHA Blast phospho-STAT3 assay from individual donors.

Supplementary Information. S2

In vitro selection of IL-23 modified RNA Aptamer

The DNA library consisted of a 40-nucleotide random region (N40) flanked by two constant regions, 5'-GGAGGGAAAAGTTATCAGGC-N_{40}-CGACGAGTAGGCTAGTCTGATGCC-3'. The template was amplified with a primer containing the T7 promoter sequence 5'-GACTGTAATACGACTCACTATAGGAGGGAAAAGTTATCAGGC-3' (underlined portion binds to DNA template). The original library was created by transcribing the double stranded DNA templates as 2'-fluoro and 2'-methoxy modified RNA with a mutant T7 RNA polymerase (Y639) to incorporate the modified nucleotides (mA, mG, fC, and fU residues). The modified RNA library was purified by polyacrylamide gel electrophoresis (PAGE).

The initial selection round contained 10^{14} molecules of library incubated at 37°C for 1 hour with 1 μM of recombinant Interleukin 23 (IL-23, from R&D Systems) in Dulbecco's Phosphate Buffered Saline with calcium chloride and magnesium chloride (DPBS++). Aptamer:pool complex was partitioned using nitrocellulose filter plates pre-treated with 0.5M KOH. Washes used DPBS++ and the selected pools were eluted from filters with urea elution buffer (7M Urea, 100 mM NaOAc, 3 mM EDTA pH 5.7). Eluted modified RNA was reverse transcribed with Thermoscript Reverse Transcriptase (Life Technologies) with the reverse primer, 5'-GGCATCAGACTAGCCTACTCGTCG-3' and amplified by polymerase chain reaction (PCR) with *Taq* polymerase and both forward and reverse DNA primers. PCR product was transcribed using the same T7 RNA polymerase above, gel purified, and put in to the subsequent round. The DNA pools from rounds were cloned into pUC19 and sequenced on an ABI 3730 sequencer to identify N40 DNA sequence of the full length IL-23 aptamer (parent; precursor to IL-23 aptamer).

Supplementary Information. S3

Dual Hybridization Assay

The dual hybridization assay (DHA) has been previously used with plasma and vitreous humour samples (Drolet et al, 2000). This assay is analogous to an ELISA where aptamer is allowed to hybridize to capture and detection DNA oligonucleotide probes. The capture probe (ARC35141; Integrated DNA Technologies) binds to the 13 nucleotides at the 5'-terminus of the aptamer and was covalently attached to magnetic beads via a 3'-terminal amino linker. The detection probe (ARC35156; Integrated DNA Technologies) was complementary to the 15 nucleotides at the 3'-terminus of the aptamer and was biotinylated at the 5'-terminus.

DHA assay plates were prepared by coating 96 well plates with 100 µL of capture probe (250 nM in 1mM EDTA/DPBS) and incubated at 4°C overnight. The capture probe solution was removed and the plate washed with 3 x 300 µL of wash buffer (Tris buffered saline with Tween; TBST) with a minimum of 1 minute soaking time for each of the 3 washes cycles and the plate was tapped out on absorbent paper after each wash. Following removal of wash buffer, 200 µL of blocking solution (5 % w/v BSA in TBST) was added to each well and the assay plate was sealed and incubated at room temperature for 60 minutes on an orbital shaker. The blocking solution was removed and the plate washed as above. A standard curve of aptamer was prepared by doubling dilutions to produce standards from 10 nM to 10 pM and DPBS as a blank sample (0 pM) was added in duplicate (60 µL per well) to a fresh 96 well plate (hybridisation plate). The extracted epidermis and dermis samples were added to the hybridisation plate (60 µL). To each well, 60 µL of the detection probes (150 nM in DPBS) was added. The final concentration of detection probes was 75 nM and aptamer standard concentrations were from 0 pM, 5 nM to 5 pM. The hybridization plate was sealed and placed in an oven at 65°C for 40 minutes to allow the aptamer to hybridise with the probes, and then allowed to cool to room temperature. One hundred µL of the aptamer standard/sample:detection probe mixture was transferred from the hybridization plate to a DHA assay plate, sealed and incubated overnight at 4°C to allow hybridization of the aptamer and capture probes. This assay solution was removed and the plate washed with TBST as above. One hundred µL of the streptavidin-poly-HRP diluted 1:20,000 with DPBS was added to the DHA assay plate, which was then sealed and incubated at room temperature for 1 hour while shaking. The streptavidin-poly-HRP solution was removed and the plate again washed with TBST before 100 µL of the TMB substrate solution (at room temperature) was added to each well; the plates were incubated at room temperature for 5 minutes until sufficient colour developed. Stop solution (100 µL) was added to each well and the plate was read at 450 nm within 30 minutes after stopping the reaction. Data analysis used Prism 5 for each plate, the background A450 value (0 pM aptamer) was subtracted from all values within the sample set. The recovered aptamer (mass per cm^2) was converted to concentration (µmol/L) in each skin layer where the volume of epidermis (cm^3) was assumed to be 0.015 cm^3 and the volume of dermis was assumed to be 0.035 cm^3. The dosing area was 1cm^2.

Supplementary Information. S4

Th17 Stimulated Human Ex-Vivo Skin Model

Cornification media: Media consisted of 237 mL of Dulbecco's Modified Eagle Medium (DMEM) with 4.0 mM L-Glutamine and without CaCl, Glucose, Sodium Pyruvate, and NaHCO3 (Invitrogen, custom order), 237 mL Ham's F-12K (Kaighn's) Medium (Gibco®, 21127-022), 1 mL 90mM Adenine, 1mL 0.94M CaCl, 1 mL 10nM Tri-iodothyronine, 1 mL Insulin-Transferrin-Selenium-Ethanolamine (ITS -X) (100X) (Gibco® 5100-056), 5 mL Antibiotic-Antimycotic (100X) (Gibco® 15240-062), 10 mL Foetal Bovine Serum (FBS) (HyCloneTM, SH30071.01HI), 5 mL GlutaMAX™ Supplement (Gibco®, 35050-061), 0.1 mL 50mg/ml Gentamicin (Invitrogen, #15750060).

Th17 Stimulation Cocktail: The cytokine cocktail was optimized to stimulate skin resident immune cells to release TH17 associated cytokines, including IL-17f and IL-22, as previously described 16. Briefly, skin was stimulated with a combination of 1 µg/ml purified NA/LE Mouse anti-human CD3 (BD Pharmingen, Cat# 555329) and 2 µg /ml anti-human CD28 (R&DSystems, Cat# MAB342), 1 µg /ml anti-Human IFN-gamma Antibody (R&DSystems, Cat#MAB2851), 1 µg/ml anti-Human IL-4 Antibody (R&DSystems, Cat# MAB304), 10 ng/ml Recombinant Human (rh) IL-1b/IL-1F2 (R&DSystems, Cat# 201-LB-025/CF), 10 ng/ml rhIL-6 (R&DSystems, Cat# 206-IL-010/CF), 1 ng/ml Recombinant Human TGF-b1 (R&DSystems, Cat# 240-B-010/CF), and rh IL-21 (Southern Biotech, Cat# 19000-00). All components were incorporated in a single mixture with the cornification media.

Tissue culture using Static Cells: Freshly excised healthy human skin was dermatomed to 750 µm and cleaned with antibiotic/antimycotic solution made up as 1% Gibco™ Antibiotic-Antimycotic (100X), 0.1% Gentamicin in 1x Dulbecco's Phosphate Buffered Saline. Twelve mm diameter biopsies were cut using disposable single-use biopsy punches (Acupunch, Acuderm, Inc) and washed in antibiotic/antimycotic solution for 5-10 minutes. Skin biopsies were placed on autoclaved 7 mm (0.38 cm^2) unjacketed static cells with 2 mL receptor volume (PermeGear, Inc; No. 6G-01-00-07-02) and a leak proof seal was maintained using metal clamps and donor chamber. The receptor chamber was filled with cornification media. Static cells were then placed in a humidified incubator at 37°C and cultured as previously described (Smith et al, 2016). First, test articles were dosed topically or systemically in the media and twenty-four hours later, the media was replaced and the Th17 stimulation cocktail was added to the receptor chamber of the Franz cells. Twenty-four hours after stimulation, the tissue was harvested, minced to less than 1x1x1 mm pieces and stored in 10x volume of RNA later (Qiagen, Cat# 76104) with 300 µL of RNeasy Lysis Buffer (Qiagen, Cat#79216) supplemented with 1% 2-Beta-Mercapto-Ethanol for RNA isolation.

Small Molecule Control: A ROR gamma inverse agonist (MW=476 g/moles) was used as a positive control at 10 µM in cornification media based on its known positive activity in the Th17 stimulated human *ex vivo* skin model (Smith et al, 2016).

RNA Isolation & Quantitation: Approximately 40 mg of minced tissue was added to homogenization tubes containing 2.8 and 1.4 mm ceramic beads. The tissue was disrupted

using a high-throughput bead mill homogenizer (Precellys®24 Atkinson, NH) at 6300 rpm for 30 seconds and 10 cycles with a 2-minute ice break. The homogenate was digested by adding 490 µL of water containing 10 µL Proteinase K (Thermo Scientific, Cat # E00491) at 55°C for 15 minutes. Digested tissue was spun down for 3 minutes at 10,000x g to pellet cell debris and the supernatant was used for RNA isolation using Qiagen's Mini RNA Isolation kit (Cat # 74106) according to the manufacturer's protocol. Total RNA was quantified using a Nanodrop 2000 (Thermo Scientific, Wilmington, DE). Isolated RNA (1.4µg) from skin tissue was used as a template in a 20 µL PCR volume using an Invitrogen SuperScript VILO cDNA Synthesis kit (# 11754-050) to create a cDNA template. The cDNA was diluted 1:25 for subsequent qPCR with the specific TaqMan probe for each gene to be quantified. A Life Technologies AVii7 PCR machine was used for the qPCR 40 amplification cycles. RNA levels of GAPDH, IL-17a, IL-17f and IL-22 relative expression were calculated using the ΔΔCT method.

RNA aptamer delivery through intact human skin

Jon D. Lenn[1], Jessica Neil[1], Christine Donahue[2], Kellie Demock[2], Caitlin Vestal Tibbetts[2], Javier Cote-Sierra[3], Susan H. Smith[4], David Rubenstein[4], Jean-Philippe Therrien[4], P. Shannon Pendergrast[5], Jason Killough[6], Marc B. Brown[7], Adrian C. Williams[8]

1) MedPharm; RTP, NC; 2) GlaxoSmithKline, R&D Platform Technology & Science, Waltham, MA; 3) Pfizer, Worldwide Research & Development; 4) GlaxoSmithKline, Center For Skin Biology; RTP, NC; 5) Ymir Genomics, Cambridge MA; 6) Momenta Pharmaceuticals, Cambridge MA; 7) Honorary Professor at University of Reading and CSO MedPharm Ltd 8) Professor of Pharmaceutics, School of Pharmacy; University of Reading

ORCID:

A.C. Williams: 0000-0003-3654-7916

Work was primarily performed in Research Triangle Park, Raleigh, North Carolina, USA.

Corresponding author:

Dr Jon Lenn

VP US Operations, MedPharm

Durham,

North Carolina

jon.lenn@medpharm.co.uk

Tel: 919-450-5673

ABBREVIATIONS: SC, stratum corneum; mAb, monoclonal antibody; log $P_{(oct/water)}$, log partition coefficient between octanol and water; SELEX, Systematic evolution of ligands by exponential enrichment; STAT, signal transducer and activator of transcription; dAb, domain antibody

ABSTRACT

It is generally recognised that only relatively small molecular weight (typically < ~500 Da) drugs can effectively permeate through intact stratum corneum. Here, we challenge this orthodoxy using a 62-nucleotide (MW=20,395) RNA-based aptamer, highly specific to the human IL-23 cytokine, with picomolar activity. Results demonstrate penetration of the aptamer into freshly excised human skin using two different fluorescent labels. A novel dual hybridisation assay quantified aptamer from the epidermis and dermis giving levels far exceeding the cellular IC_{50} values (> 100,000-fold) and aptamer integrity was confirmed using an oligonucleotide precipitation assay. A Th17 response was stimulated in freshly excised human skin resulting in significantly upregulated IL-17f, and 22; topical application of the IL-23 aptamer decreased both IL-17f and IL-22 by approximately 45% but did not result in significant changes to IL-23 mRNA levels, confirming that the aptamer did not globally suppress mRNA levels. This study demonstrates, for the first time, that very large molecular weight RNA aptamers can permeate across the intact human skin barrier to therapeutically relevant levels into both the epidermis and dermis and that the skin penetrating aptamer retains its biologically active conformational structure capable of binding to endogenous IL-23.

INTRODUCTION

It is widely accepted that the intact stratum corneum (SC) provides the primary barrier to topical and transdermal drug delivery and so restricts the therapeutic targets that can be accessed topically. Relatively few molecules have the appropriate physicochemical and therapeutic properties to allow topical and transdermal administration. It is generally recognised that only relatively small molecular weight (typically <500 Da) and moderately lipophilic (log $P_{(oct/water)}$ 1-3.5) drugs can effectively permeate through the SC (Bos and Meinardi, 2000; Williams, 2003).

The introduction of biological therapeutic agents has revolutionised the treatment of psoriasis, a chronic inflammatory skin disorder. Although effective when delivered systemically, the large size of proteins, including monoclonal antibodies, domain antibodies, and even Fab fragments, is thought to preclude their development as topical medicines. Aptamers are oligonucleotide-based molecules that can specifically bind to proteins or other cellular targets; aptamers have been approved for macular degeneration, and others are in clinical development for cancer, haemophilia, anaemia, and diabetes (Darisipudi et al, 2011; Ng et al, 2006; Parunov et al, 2011; Schwoebel et al, 2013). Aptamers offer a significant advantage over antisense molecules because their structure and composition can be modified while retaining pharmacological activity and they possess conformational plasticity and flexibility (Nomura et al, 2010). Systematic evolution of ligands by exponential enrichment (SELEX) has accelerated the discovery and development of aptamers allowing functional isolation of oligonucleotides against specific targets that could be used to treat skin diseases (Keefe et al, 2010).

Psoriasis is driven by activated T cells (Di Cesare et al, 2009). Elevated levels of IL-23 and Th17-related cytokines in lesional skin biopsies encouraged targeting of the IL-23/Th17 pathway for psoriasis treatment (Blauvelt, 2008). Ustekinumab, a human IgG1κ monoclonal antibody (mAb) that binds to the p40 protein subunit of IL-12 and IL-23 cytokines, is approved for moderate/severe plaque psoriasis. However, there are risks associated with long term systemic p40 inhibition given the role of IL-12 in intracellular microbial response and tumour suppression (Koutruba et al, 2010; Tausend et al, 2014). To circumvent this, a human mAb specifically directed against IL-23 gave positive clinical responses in patients with

moderate-to-severe psoriasis, suggesting that neutralizing IL-23 alone is a promising psoriasis therapy (Sofen et al, 2014).

We have developed and optimized an aptamer that is a first-in-class inhibitor of IL-23 for topical treatment of psoriasis (Figure 1). This water-soluble 62-nucleotide (MW=20,395) aptamer has high affinity and specificity to human IL-23 cytokine. Employing a well-validated model, it has been shown for the first time that, *without* physically disrupting the SC, this large molecular weight RNA based aptamer can penetrate into and permeate through human skin. Novel analyses to extract, detect and quantify the macromolecule in human skin showed the IL-23 aptamer was present at therapeutically relevant levels. Finally, delivery was confirmed through a cytokine induced inflammatory *ex vivo* human skin model (Smith, et al, 2016). This is the first study showing the passive delivery of a large molecular weight aptamer across intact human skin.

RESULTS

The IL-23 aptamer is biologically active

Biological activity of the aptamer was confirmed in three different assays. Inhibition of IL-23 dependent stimulation of STAT3 activity in PHA-Blast cells showed that the 61-mer minimer (IC_{50} 0.075 nM ± 0.030 nM) was more potent than the parent full length (84-mer) IL-23 aptamer (IC_{50} 0.26 nM ± 0.036 nM); the activity of both aptamers was greater than the control anti-p19 antibody (IC_{50} 0.69 nM ± 0.12 nM). Secondly, the aptamer blocked endogenous IL-23 activation in PHA/IL-2 activated T-cells, evaluated by measuring levels of phospho-STAT3. Finally, the IL-23 aptamer did not inhibit IL-12 activation of PHA/IL-2 activated T-cells; many IL-23 antagonists also inhibit IL-12 since they share the p40 subunit but our IL-23 aptamer only inhibits IL-23 activation and not IL-12 activation, similar to the anti-p19 antibody. Experimental methods and representative inhibition curves can be found in Supplementary Information (S1).

The IL-23 aptamer penetrates human skin

Passive penetration of topically applied IL-23 (20.4 kDa) aptamer through human skin was assessed using freshly excised skin with and without a fully functional stratum corneum barrier (Figure 2a). Fluorescently labelled IL-23 aptamer (21.4 kDa) was formulated in an oil-in-water cream vehicle previously described to aid delivery of macromolecules (Mehta et al, 2000). A finite dose (10 mg/cm^2 of formulation containing 1% aptamer) was applied to

skin mounted in flow-through diffusion cells. To ensure the washing procedure effectively removed residual aptamer from the skin surface and to assess tissue auto fluorescence, the medicated cream was applied and immediately removed (zero hour sample). No fluorescence in intact or partially compromised skin confirmed the washing procedure effectively removed residual aptamer from the skin surface. Interestingly, skin with the SC removed allowed permeation at this zero hour sample suggesting the aptamer permeates through the viable epidermis almost immediately and is not further limited by tight junctions in the epidermis. In contrast, a single domain antibody (dAb) fragment (13.1 kDa) failed to permeate into the viable epidermis of tape stripped skin (Figure 2b) demonstrating that these junctions can regulate passive diffusion of large molecular weight biological agents. After four hours of topical exposure, the IL-23 aptamer penetrated not only fully and partially compromised tissue, but also through intact human skin, with an intensity gradient decreasing from the skin surface to the basement membrane. Interestingly, after dosing full thickness intact skin, no aptamer was detected in the receiver solution but rather the macromolecule appears to be retained in the tissue, perhaps via cellular uptake (see below).

To confirm that the aptamer indeed penetrated the skin and that fluorescence was not simply due to dissociation of the label, the IL-23 aptamer was extracted from non-compromised (Unt) and partially compromised (Abr) skin samples, visualized fluorescently on a polyacrylamide gel and compared to the IL-23 aptamer dylight 488 standard (IL-23 aptamer) and a 28-mer SDF-1 aptamer (28-mer) (Figure 2c). Concordance of skin extracted aptamer with the IL-23 aptamer dylight 488 standard shows delivery of intact labelled macromolecules to these skin layers, providing evidence that the fluorescence images are not from dissociation of the label though this cannot be fully discounted from the images in (a) and (b) alone.

Delivery into intact human abdominal skin with longer exposures using a second fluorescent label (Cy3) was also performed in order to evaluate cellular uptake, but with dosing of the IL-23 aptamer from an aqueous vehicle. Again the wash procedure removed aptamer from the skin surface (zero hour samples), confirming that fluorescence in the tissue results from topical penetration through the intact barrier (Figure 3). The IL-23 aptamer penetrated intact skin within 6 hours with fluorescence intensity increasing up to 24 hours. Fluorescence was detected in the extracellular matrix, as seen by the fluorescent gradient through the viable epidermis, and intracellular, confirmed by confocal imaging with fluorescence (potentially

within the nucleus) of keratinocytes in the *ex vivo* skin sections. This accords with anti IL-17A RNA aptamer uptake by cultured cells (Doble et al, 2014). Importantly, the distribution of the IL-23 aptamer suggests that topically delivered aptamers could modulate both intracellular and extracellular targets in the skin.

Detection and Quantitation of IL-23 aptamer in human skin

The fluorescence images suggest topical delivery of RNA aptamers through intact SC. As the current paradigm is that biomacromolecules cannot penetrate intact human skin, a dual hybridization assay (DHA) was developed where detection and capture probes quantified IL-23 aptamer extracted from the skin. The DHA selectivity and sensitivity was systematically verified through removal of nucleotides from both 5' and 3' ends of the aptamer and the capture/detection probes; single nucleotide removals resulted in loss of detection. Complete loss was observed when two or more nucleotides were removed at the expected skin concentration of <1,000 pM. The IL-23 aptamer was formulated into both cream and microemulsions, suggested as optimal vehicles for topical delivery of peptides and proteins (Russell-Jones and Himes, 2011), applied to freshly excised human skin mounted in flow through diffusion cells and removed at 0, 6 and 24 hours. The epidermis was removed by heat-separation (the temperature of which has been previously shown not to damage the aptamer) to allow extraction and quantification of the IL-23 aptamer in both the epidermis and dermis. Very low concentrations of IL-23 aptamer (0.09 – 0.36 µg) were in the epidermis and dermis after the initial (control) washing procedure (Figure 4a) but these levels were subtracted from the six and twenty four hour treated samples to account for any aptamer remaining after the wash procedure (Figure 4b).

Both vehicles delivered IL-23 aptamer to concentrations that exceeded by several orders of magnitude the desired cellular IC_{50} into both the epidermis and dermis, with delivery increasing in a time dependent fashion (Figure 4b). Interestingly, the cream delivered more aptamer compared to the microemulsion; 3.4 and 5.5 fold greater levels in the epidermis and dermis respectively following 6 hours of application ($P<0.009$ epidermis and $P<0.06$ dermis) with 1.5 (epidermis) and 2.3 fold (dermis) increases after 24 hours treatment ($P<0.06$ epidermis and $P<0.04$ dermis). The cream delivered 4 µg (14 µM, 4% of the applied aptamer dose) and 12 µg (37 µM, 12% of the applied dose) of IL-23 aptamer into the epidermis after 6 and 24 hour treatment respectively, which is approximately 43,000 and 119,000-fold above the cellular IC_{50} as shown in STAT3 activation of primary human T-cells (Figure 1e). The

cream delivered 0.6 µg (0.9 µM, 0.6% of the applied aptamer) and 0.7 µg (1.2 µM, 0.7% of the applied dose) to the dermis after 6 or 24 hours respectively, i.e. some 2,500 and 3,400 fold above the cellular IC_{50} for the IL-23 aptamer. In parallel, aptamer was also applied from an aqueous (control) solution at 10 mg/cm^2 but provided lower delivery; for example, 6 h post dose, 0.3 and 0.1 µg of the aptamer was detected in the epidermis and dermis respectively.

To demonstrate that the aptamer did not degrade during transit through the skin, an oligonucleotide precipitation assay using the DHA capture probes extracted the IL-23 aptamer from skin and was then visualized by polyacrylamide gel electrophoresis. The extracted RNA bands aligned with the IL-23 aptamer standards. Further, the relative band intensities correlated with the quantified values from the above DHA. Similar to the relative aptamer levels delivered by the two vehicles in the DHA, a more intense band was visualized for the cream compared to the microemulsion (Figure 4c and d).

Topical application of IL-23 aptamer inhibits Th17 derived cytokines in human skin

The above studies demonstrate that therapeutically relevant levels of aptamer can be delivered to, and recovered from, intact human epidermal and dermal tissue. An *ex vivo* human Th17 polarized skin model was used to further confirm delivery and intrinsic pharmacodynamics of this aptamer. Freshly excised human skin was mounted in static cells with growth media as the reservoir, and the skin was stimulated to induce a Th17 response (Smith, et al, 2016). The activity of the topically delivered IL-23 aptamer in the skin was compared to a basolateral treatment with IL-23 aptamer and an ROR gamma inverse agonist. The Th17 stimulating conditions significantly upregulated IL-17f, and 22 (Figure 5). Topical application of the IL-23 aptamer (1% aqueous solution of IL-23) decreased both IL-17f and IL-22 by approximately 45% ($p<0.001$ and 0.05 respectively) similar to those observed when IL-23 aptamer was included in the media (10µM IL-23). The addition of IL-23 aptamer, either topically or basolaterally, did not result in significant changes to IL-23 mRNA levels, confirming that the aptamer was not globally suppressing mRNA levels, but was specific for IL-17f and IL-22. Interestingly, the reduction of IL-22 mRNA following topical application of IL-23 aptamer was similar to that of the small molecule ROR gamma inverse agonist. These results confirm that skin penetrating aptamer retains the biologically active conformational structure capable of binding to endogenous IL-23.

DISCUSSION

In general, the literature does not support the ability of large molecules, particularly biomacromolecules, to significantly transit the stratum corneum passively to gain entry into the skin. Here, it is demonstrated that a 62-nucleotide (MW=20,395) mRfY aptamer not only transits the SC, but does so to therapeutically relevant levels in the epidermis and dermis. Multiple approaches demonstrate passage through the intact SC into the viable epidermis, including (i) fluorescently labelled aptamer (using two different labels) confirmed with gel electrophoresis, (ii) confocal microscopy, and (iii) dual hybridization assay using capture and detection probes with oligonucleotide precipitation. In contrast, topically administered domain antibodies failed to penetrate the SC or enter the viable epidermis. The aptamer within skin far exceeded the desired cellular IC_{50} values (119,000-fold > IC_{50} in the epidermis; 3,400-fold > IC_{50} in the dermis) following 24 h delivery from a simple cream formulation. Additionally, intracellular and extracellular localization was observed. Nonspecific uptake of an RNA aptamer into primary human keratinocytes has been previously reported (Doble et al, 2014), though the authors noted that site-specific (i.e., topical) treatment to reduce inflammatory mediators produced by deeper keratinocytes would be problematic due to aptamer uptake by upper skin layer keratinocytes. In our studies, topically delivered IL23 aptamer suppressed IL-17 and IL-22 mRNA production in a cytokine stimulated *ex vivo* human skin model, showing that the aptamer is available to exert a therapeutic effect in deeper skin layers confirming the fluorescence, dual hybridization assay, and oligonucleotide precipitation assay data.

There are conflicting reports on the feasibility of topical delivery of antisense oligonucleotides, though notably none are clinically approved (Butler et al, 1997; Mehta et al, 2000; White et al, 1999; White et al, 2002). Aptamers are a relatively new class of oligonucleotide-based technologies that can bind to a wide range of molecules and have been mainly used for diagnostics and systemic therapeutics. In contrast to antisense oligonucleotides, aptamers offer significant conformational plasticity and flexibility (Nomura et al, 2010). The structure and composition of aptamers can be modified but retain significant activity, whereas modifications to antisense molecules are avoided because of their potential impact on efficacy. The literature reports rapid systemic clearance of aptamers, limiting unwanted side effects and restricting the biologic effects of topically

administered aptamers to the skin (Healy et al, 2004; Watson et al, 2000). Thus, RNA aptamers represent a broad class of biological compounds that could be used for local targeting of skin diseases.

Since our results contradict the "normal" rules governing molecular properties and topical drug delivery, numerous potential mechanisms by which the aptamer enters the tissue were explored (and will be described in detail in a further publication). However, the role of water was probed by hydrating the stratum corneum for 12 h prior to dosing and by occluding (or not) the both pre-hydrated and none pre-hydrated tissue, using finite (5-10 mg/cm^2) and infinite (300 mg/cm^2) doses of the aptamer in an aqueous vehicle alongside blank controls for detection at 6 and 15 h in the epidermis and dermis, as above. In short, the water gradient across skin was removed by fully hydrating or occluding the stratum corneum; pre-hydrating the tissue was broadly detrimental but occlusion was generally beneficial, most notably for infinite dosing of none pre-hydrated skin. Delivery of this highly water soluble aptamer thus appears to be influenced by changing the water gradients across the skin.

Since the conformational structure of aptamers can be disrupted by metal ions (notably Ca^{2+} and Mg^{2+}) that are present in human skin, aptamer delivery from aqueous vehicles was compared to delivery when the vehicle included 100 or 10 mM EDTA, or when 10 mM $CaCl_2$ or 10 mM $MgCl_2$ was added; similar studies also used these adjuncts in the receiving fluid. Neither chelating the ions with EDTA nor adding additional ions significantly impacted aptamer amounts in either the dermis or epidermis at 6 or 15 h post dosing.

Though active transport mechanisms are widely regarded as absent in the stratum corneum, it is feasible that some carrier systems may operate in the deeper skin layers. This was explored by comparing aptamer delivery at 4 and 32°C; amounts in the dermis and epidermis at 6 and 15 h post dosing were invariant with temperature confirming passive rather than active transport.

The optimised IL-23 aptamer is folded and the role of the secondary structure in its skin penetration was explored through comparison with a series of four variants containing secondary or tertiary modifications. 24 hour post dosing, all variants were detected in the epidermis; approximately 10% of the applied dose of the optimised aptamer was detected

whereas 17 – 5% of the variants doses were detected in this layer. Different IL-23 aptamers with a range of molecular weights (from an 85-mer, mw = 28,950 Da to a 39-mer, mw = 13,435) were applied alongside a second series of aptamers against the transferrin receptor (85-mer, mw = 29,348; 45-mer, mw = 15,512; 36-mer, mw = 12,486). Fluorescence imaging showed that all the RNA-based aptamers penetrated into intact human skin and were visualised within the epidermis. In contrast to small "conventional" drugs, no molecular weight dependence on uptake was seen for the aptamers and, as a class, they appear to be able to penetrate the stratum corneum.

In summary, numerous mechanisms for aptamer uptake into intact human have been explored. From the fluorescence images, there is no evidence to suggest that delivery is principally via the shunt routes. For the large RNA-based structures, uptake is independent of molecular weight (between 12.5 and 29.3 kDA) and was unaffected by our secondary and tertiary conformational modifications. There is no evidence for active transport and divalent cation effects were not detected. Some delivery-dependence on tissue water content is seen, perhaps not surprisingly considering that these molecules are highly water soluble, but pre-hydrating the skin was detrimental whereas occlusion was generally beneficial.

For the first time, this study demonstrates that, despite being very large molecular weight biotherapeutic agents, RNA aptamers can permeate across the intact human skin barrier to therapeutically relevant levels in both the epidermis and dermis.

MATERIALS AND METHODS

IL-23 Aptamer

Following in vitro selection (Supplementary Information S2), the IL-23 aptamer was fully minimized and optimised from 84 to 61 nucleotides using computational folding prediction programs and systematic deletion. Modifications at the 2' position of the sugar for each base were evaluated to improve activity as well as predicted in vitro stability either by substitution of a 2'Fluoro with a 2′-O-methoxyethyl(2'OME) (2'F -> 2'OMe) or substitution of a 2′-O-methoxyethyl with a 2'Fluoro (2'OMe->2'F). All tolerated or potency increasing substitutions were combined with all tolerated deletions within the oligonucleotide. Appendage of a 3'-inverted thymidine residue, to increase nuclease resistance, resulted in a 62 nucleotide long molecule (IL-23 aptamer) composed of ten 2'-O-methyladenosines (mA),

one 2'-fluoroadenosine (fA), fourteen 2'-Omethylguanosines (mG), six 2'-fluoroguanosines (fG), three 2'-O-methylcytosines (mC), thirteen 2'-fluorocytosines (fC), one 2'-O-methyluridine (mU), thirteen 2'-fluorouridines (fU) and the 3'-terminus is capped with a single inverted deoxythymidine residue to protect against nuclease degradation (MW= 20,395). The IL-23 RNA mRfY aptamer was conjugated with dylight 488 or Cy3 fluorescent labels as an amide conjugate during chemical synthesis.

Preparation of Human *Ex Vivo* Skin

Full-thickness human skin was obtained within several hours from patients undergoing elective abdominoplasty. The acquisition, informed consent form (IFC), and protocol for use were approved by an independent Investigational Review Board (Pearl IRB, Indianapolis, IN). Immediately after collection, the skin was transferred to phosphate buffered saline (PBS) and kept at 4°C during transit. Subcutaneous fat was removed from the samples and the skin rinsed briefly in Hank's balanced salt solution with 1% antibiotic/antimycotic. Split-thickness dermatomed skin was prepared by placing full thickness skin on high-density foam blocks and cut to specified thickness (250 ± 100 μm, 500 ± 100 μm, or 750 ± 100 μm) using an Electro-Dermatome.

Skin was left untreated for uncompromised barrier (intact), pre-treated with sodium bicarbonate crystals to partially disrupt the barrier (abraded), or pre-treated with approximately 28 tape strips to completely remove the barrier (tape stripped). To confirm SC disruption, skin sections immediately after treatments were fixed in formalin and paraffin-embedded, sectioned and stained with H&E.

In Vitro Skin Penetration

Two different flow-through diffusion cells (PermeGear, Inc and Eclectech, Inc.) or static diffusion cells (PermeGear, Inc) were used to assess aptamer permeation and activity.

Flow through diffusion system: Flow-through diffusion cells were placed in cell warming supports to maintain the skin surface temperature at 32 ± 2°C. Cells were connected to multi-channel peristaltic pumps via Tygon® tubing, and the cell outlets were fitted with poly ether ether ketone (PEEK) tubing, angled to drip into 96-well plates or 20 mL vials on fraction collectors. Dermatomed *ex vivo* human skin was mounted in the diffusion cells, SC side up. Donor compartment blocks placed on the skin were secured to provide a leak proof seal, exposing a surface area of 1.0 cm^2. The pumps were adjusted to maintain sink conditions

with a flow-rate of 0.300 mL/hour (5.0 µL/minute) or 3.6 mL/hour (60 µL/minute) for the ChanneL cells and PermeGear Cells respectively with phosphate buffered saline used as the receiving fluid. Both systems were allowed to equilibrate for ~30 min prior to dosing.

Static diffusion cell system: Static (Franz-type) cells were used for the Th17 stimulated human ex-vivo skin model. Briefly, dermatomed *ex vivo* skin was mounted SC side up on static diffusion cells with an average surface area of approximately 0.6 cm² and a receiver compartment volume of approximately 2.0 mL. The receiver chamber was initially filled with cornification media and incubated at 37°C. Then skin was dosed topically or systemically (in the media) with aptamer for twenty-four hours before the receiver solution was replaced with Th17 stimulation cocktail. Twenty-four hours after stimulation, the tissue was harvested, minced before RNA isolation and quantitation. Full details can be found in Supplementary Information S4.

Dosing and vehicles: The IL-23 aptamer was formulated at 1% in either an oil-in-water cream (62.5% Di water, 0.5% Benecel MP333C, 10% Isopropyl Myristate, 10% Glyceryl Monostearate NSE 400, 15% Polyoxyl-40-stearate, and 1% Phenonip), microemulsion (5% Isopropanol, 20% Di water, 1.5% benzyl alcohol, 30% Drakeol-5, 15% Brij 02, 15% Brij 010, 12.5% cetrimonium chloride) or water vehicle (controls; 98.9% DI Water, 0.1% Polysorbate 20, 1% Benzoyl alcohol). The formulations were uniformly dosed onto the SC surface using a positive displacement pipette, set to deliver 10 mg/cm^2. The donor chambers were left open to ambient conditions, i.e., the skin was not occluded.

Post-dosing skin washing and isolation: At predetermined time points (0, 4, 6, 15, or 24 hours), the skin was thoroughly cleansed. Three cotton buds; dry, wet (1:9 Hexane:MeOH or 0.05% Tween 20 in PBS) and dry were used to remove the surface formulation and was immediately followed by 3 consecutive tape strips (Scotch® Transparent Tape 175L-WG). These samples were not analysed and considered as surface deposited compound, i.e. not penetrating the skin. Heat separation of skin layers by soaking in hot water was avoided to prevent migration of aptamer or biomarkers. Thus, post treatment, the skin was placed in an oven at 60°C for 2 minutes, and the epidermis was carefully separated from the dermis using forceps. Epidermis and dermis samples analysed by the dual hybridization assay (DHA) were placed into separate vials and 1 mL of 0.25 % trypsin was added to each. Vials were

placed in an oven set at 37°C for 16 to 20 hours and then the extraction diluent was removed and centrifuged at 13,000 RPM for 10 minutes to remove residual materials.

Conjugated Fluorescence Detection

Dried skin (cleaned as above) was placed epidermis side down on a clean cutting board and smaller sections cut with a clean razor blade to avoid carry over. Sections were placed on edge in 15x15 mm moulds and immediately frozen in OCT using an isopentane/dry ice bath. Moulds were then wrapped in aluminium foil, and stored at -80°C. For immunofluorescence (IFC), the frozen blocks were placed into a -20°C cryostat 3 minutes prior to sectioning. Five µm sections were cut and mounted on individual Richard Allen Bond-Rite slides which were fixed in -20˚C acetone for 10 minutes and then air dried for 30 minutes. Slides were rinsed three times with Tris Buffered Saline (TBS) (Dako). Slides with nuclear staining were cover-slipped with ProLong® Gold Antifade Reagent with diamidino-2-phenylindole (DAPI) (Invitrogen). Permeation was assessed using a fluorescence microscope fitted with appropriate filters for the fluorophore. Images were taken using a Leica DMRXA2 microscope mounted with a Nikon DS-QiMc monochromatic camera and NIS Elements BR 3.2 software. For each independent experiment, skin was also dosed with vehicle alone (control) and all pictures were taken using the same exposure time to discard auto-fluorescence signals from skin or fluorescence from residual vehicles.

Dual Hybridization Assay

The dual hybridization assay (DHA) has been previously used with plasma and vitreous humour samples (Drolet et al, 2000). This assay is analogous to an ELISA where aptamer is allowed to hybridize to capture and detection DNA oligonucleotide probes. The capture probe (ARC35141; Integrated DNA Technologies) binds to the 13 nucleotides at the 5'-terminus of the aptamer and was covalently attached to magnetic beads via a 3'-terminal amino linker. The detection probe (ARC35156; Integrated DNA Technologies) was complementary to the 15 nucleotides at the 3'-terminus of the aptamer and was biotinylated at the 5'-terminus. Further details are available in the accompanying Supplementary Information (S3)

The recovered aptamer (mass per cm^2) from each skin layer was converted to concentration (µmol/L) where the volume of epidermis was assumed to be 0.015 cm^3 and the volume of dermis was assumed to be 0.035 cm^3.

Oligo-Protein Precipitation Assay

To confirm aptamer quantitation by DHA, a new assay was developed, termed oligo-precipitation "OP". This used the same biotinylated capture primers from the DHA to mix with the 100 μL of digested skin samples (epidermis or dermis). Samples were heated and cooled to allow primer to hybridize. Streptavidin beads were added to pull down the aptamer-primer complex. The aptamer was then eluted off the beads, loaded onto a 15% urea gel and stained with Sybr Gold to visualize and compare aptamer bands.

Th17 Stimulated Human *Ex Vivo* Skin Model

Th17-skewed cytokine expression was induced from *ex vivo* skin-resident immune cells according to our earlier report demonstrating efficacy of a novel RORγ inverse agonist small molecule (Smith et al, 2016). Details can be found in Supplementary Information (S4).

CONFLICT OF INTEREST

At the time of the study, Jon Lenn, Jessica Neil, Christine Donahue, Kellie Demock, Caitlin Vestal Tibbetts, Susan H. Smith, David Rubenstein and Jean-Philippe Therrien were employees of GlaxoSmithKline; Javier Cote-Sierra was employed by Pfizer; P. Shannon Pendergrast was employed by Ymir Genomics; Jason Killough was employed by Momenta Pharmaceuticals; Marc Brown was employed by MedPharm.

ACKNOWLEDGEMENTS:

Madaline Gilbert for work on the endogenous IL-23 production. Kofi Nyam, Ayesha Paul, and Bhasha Desai worked on the skin penetration studies. Michael Luke, Mary Larm, Leon Loupenok developed the IL-23 cream and microemulsion formulations. Charlotte Stewart, Rob Turner, and Jennifer Nelson for help with the DHA analysis. Robert Hale, Christopher Arico-Muendel for their help with labelled aptamers. Beth Millerman for histological sections. Thi Bui, and Kathleen Richter for their help with the development of the target engagement *ex vivo* skin model.

REFERENCES

Blauvelt A. T-helper 17 cells in psoriatic plaques and additional genetic links between IL-23 and psoriasis. J Invest Dermatol 2008; 128:1064-1067.

Bos JD, Meinardi MM. The 500 Dalton rule for the skin penetration of chemical compounds and drugs. Exp Dermatol 2000; 9:165-169.

Butler M, Stecker K, Bennett CF. Cellular distribution of phosphorothioate oligodeoxynucleotides in normal rodent tissues. Lab Invest 1997; 77:379-388.

Darisipudi MN, Kulkarni OP, Sayyed SG, Ryu M, Migliorini A, Sagrinati C et al. Dual blockade of the homeostatic chemokine CXCL12 and the proinflammatory chemokine CCL2 has additive protective effects on diabetic kidney disease. Am J Pathol 2011; 179:116-124.

Di Cesare A, Di Meglio P, Nestle FO. The IL-23/Th17 axis in the immunopathogenesis of psoriasis. J Invest Dermatol 2009; 129:1339-1350.

Doble R, McDermott MF, Cesur O, Stonehouse NJ, Wittmann M. IL-17A RNA aptamer: possible therapeutic potential in some cells, more than we bargained for in others? J Invest Dermatol 2014; 134:852-855.

Drolet DW, Nelson J, Tucker CE, Zack PM, Nixon K, Bolin R, et al. Pharmacokinetics and safety of an anti-vascular endothelial growth factor aptamer (NX1838) following injection into the vitreous humor of rhesus monkeys. Pharm Res 2000; 17:1503-1510.

Healy JM, Lewis SD, Kurz M, Boomer RM, Thompson KM, Wilson C, et al. Pharmacokinetics and biodistribution of novel aptamer compositions. Pharm Res 2004; 21:2234-2246.

Keefe AD, Pai S, Ellington A. Aptamers as therapeutics. Nat Rev Drug Discov 2010; 9:537-550.

Koutruba N, Emer J, Lebwohl M. (2010) Review of ustekinumab, an interleukin-12 and interleukin-23 inhibitor used for the treatment of plaque psoriasis. Ther Clin Risk Manag 2010; 6:123-141.

Mehta RC, Stecker KK, Cooper SR, Templin MV, Tsai YJ, Condon TP, et al. Intercellular adhesion molecule-1 suppression in skin by topical delivery of anti-sense oligonucleotides. J Invest Dermatol 2000; 115(5):805-812.

Ng EW, Shima DT, Calias P, Cunningham ET Jr, Guyer DR, Adamis AP. Pegaptanib, a targeted anti-VEGF aptamer for ocular vascular disease. Nat Rev Drug Discov 2006; 5:123-132.

Nomura Y, Sugiyama S, Sakamoto T, Miyakawa S, Adachi H, Takano K, et al. Conformational plasticity of RNA for target recognition as revealed by the 2.15 A crystal structure of a human IgG-aptamer complex. Nucleic Acids Res 2010; 38:7822-7829.

Parunov LA, Fadeeva OA, Balandina AN, Soshitova NP, Kopylov KG, Kumskova MA, et al. Improvement of spatial fibrin formation by the anti-TFPI aptamer BAX499: changing clot size by targeting extrinsic pathway initiation. J Thromb Haemost 2011; 9:1825-1834.

Russell-Jones G, Himes R. Water-in-oil microemulsions for effective transdermal delivery of proteins. Expert Opin Drug Deliv 2011; 8:537-546.

Schwoebel F, van Eijk LT, Zboralski D, Sell S, Buchner K, Maasch C et al. The effects of the anti-hepcidin Spiegelmer NOX-H94 on inflammation-induced anemia in cynomolgus monkeys. Blood 2013; 121:2311-2315.

Smith S, Carlos E, Peredo CE, Yukimasa Takeda Y, Bui T, Neil J, Rickard D et al. Development of a Topical Treatment for Psoriasis Targeting RORγ: From Bench to Skin. PLOS ONE, doi: 10.1371/journal.pone.0147979.

Sofen H, Smith S, Matheson RT, Leonardi CL, Calderon C, Brodmerkel C et al. Guselkumab (an IL-23-specific mAb) demonstrates clinical and molecular response in patients with moderate-to-severe psoriasis. J Allergy Clin Immunol 2014; 133:1032-1040.

Tausend W, Downing C, Tyring S. Systematic review of interleukin-12, interleukin-17, and interleukin-23 pathway inhibitors for the treatment of moderate-to-severe chronic plaque psoriasis: ustekinumab, briakinumab, tildrakizumab, guselkumab, secukinumab, ixekizumab, and brodalumab. J Cutan Med Surg 2014; 18:156-169.

Watson SR, Chang YF, O'Connell D, Weigand L, Ringquist S, Parma DH. Anti-L-selectin aptamers: binding characteristics, pharmacokinetic parameters, and activity against an intravascular target in vivo. Antisense Nucleic Acid Drug Dev 2000; 10:63-75.

White PJ, Fogarty RD, Liepe IJ, Delaney PM, Werther GA, Wraight CJ. Live confocal microscopy of oligonucleotide uptake by keratinocytes in human skin grafts on nude mice. J Invest Dermatol 1999; 112:887-892.

White PJ, Gray AC, Fogarty RD, Sinclair RD, Thumiger SP, Werther GA, et al. C-5 propyne-modified oligonucleotides penetrate the epidermis in psoriatic and not normal human skin after topical application. J Invest Dermatol 2002; 118:1003-1007.

Williams AC. Transdermal and Topical Drug Delivery: from Theory to Clinical Practice, Pharmaceutical Press, London, UK 2003; 242.

Wingens M, Pfundt R, van Vlijmen-Willems IM, van Hooijdonk CA, van Erp PE, Schalkwijk J. Sequence-specific inhibition of gene expression in intact human skin by epicutaneous application of chimeric antisense oligodeoxynucleotides. Lab Invest 1999; 79:1415-1424.

FIGURE LEGENDS

Figure 1. Predicted secondary structure of the fully minimised and optimized IL-23 aptamer using mfold.

Figure 2. Penetration of IL-23 aptamer through compromised and uncompromised human skin. (a). Penetration of IL-23 dylight 488 labelled aptamer (green) into intact, abraded and tape stripped human abdominal skin showing aptamer distribution after washing from the skin surface immediately after dosing (wash control) and 4 hours post dosing. (b) Distribution of a single domain fully human antibody (dAb) fragment (13.1 kDa) dosed topically onto tape stripped skin. (c) Polyacrylamide gel of fluorescent aptamer extracted from intact (untreated, UNT) and abraded (Abr) skin compared to IL-23 aptamer dylight 488 standard (IL-23 Aptamer) and a 28-mer SDF-1 aptamer (28-mer).

Figure 3. Topically applied IL-23 aptamer penetrates human skin and into keratinocytes. (a) Penetration of IL-23 Cy3 labelled aptamer (orange) into intact human abdominal skin after zero (wash control), 6 and 24 hours post dosing. (b). Uptake of IL-23 aptamer into skin keratinocytes (dashed lines indicating the epidermal junction). (c) Intracellular uptake of aptamer (green) with nuclear DAPI stain (blue) used for cellular orientation.

Figure 4. Dual Hybridization Assay (DHA) and Oligonucleotide Precipitation to quantify intact aptamer within skin. (a) Aptamer recovery by DHA from epidermis following zero (wash control), 6 and 24 hours application from a microemulsion and cream formulation. (b) Aptamer recovery by DHA from dermis following zero (wash control), 6 and 24 hours application from a microemulsion and cream formulation. (c) Polyacrylamide gel of aptamer extracted from the epidermis by oligonucleotide precipitation following dosing from a cream (Crm) compared to the IL-23 aptamer standard (Std=80 ng). (d) Polyacrylamide gel of aptamer extracted from the dermis by oligonucleotide precipitation following dosing from a cream (Crm) and microemulsion (ME) compared to IL-23 aptamer standards (40ng, 20ng, 10ng, 5ng, 2.5ng, 1.25ng, 0.6ng). DHA data shown as mean ± SEM, n=5.

Figure 5. Topical application of IL-23 aptamer inhibits Th17 derived cytokines in human skin. Freshly excised human abdominal skin was mounted and clamped in place using static cells containing growth media and stimulated twenty four hours later to induce a Th17 response. The skin was treated topically twice with 8 µL of IL-23 aptamer (210 µg/cm2) in an aqueous vehicle before and concurrent with Th17 stimulation. IL-23 aptamer (10 µM) and a RORgamma inverse agonist (10 µM; small molecule) was included in the media as systemic controls. Twenty-four hours post stimulation, skin was harvested and relative transcript levels of Th17-type cytokines, IL-17f (a), IL-22 (b), and IL-23 (c) were determined by qPCR. Bars represent the mean percent of maximum stimulation (set to 100%) from 3 different skin donors (n=3).

Figure 1. Predicted secondary structure of the fully minimised and optimized IL-23 aptamer using mfold

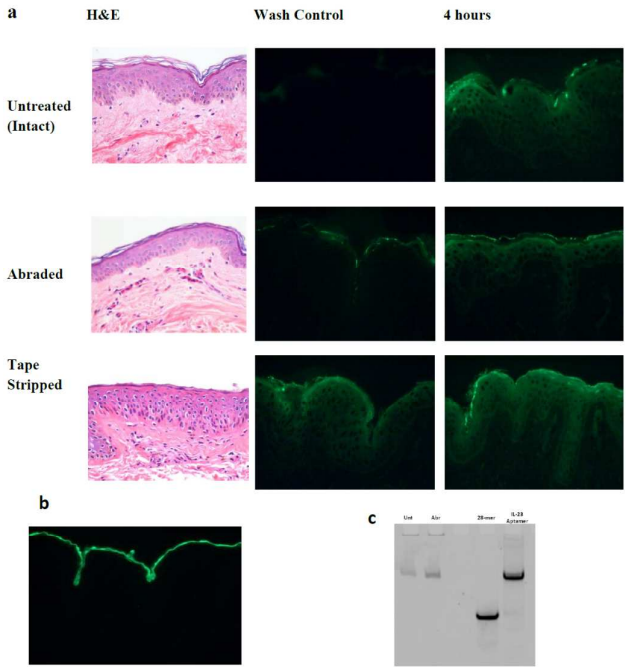

Figure 2. Topical application of IL-23 aptamer penetrates compromised and uncompromised human skin.

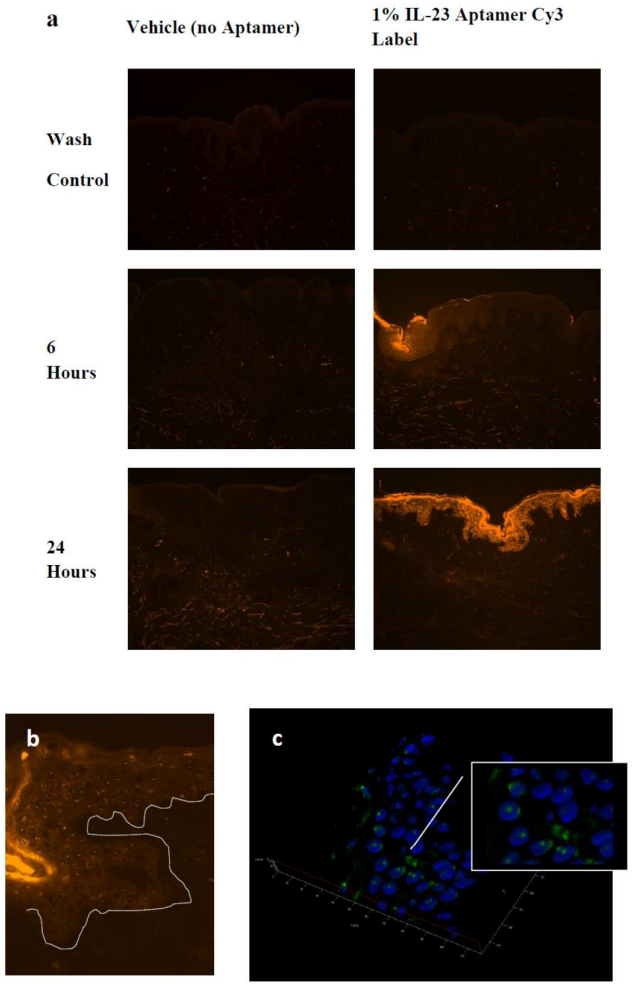

Figure 3. Topical application of IL-23 aptamer penetrates human skin and into keratinocytes.

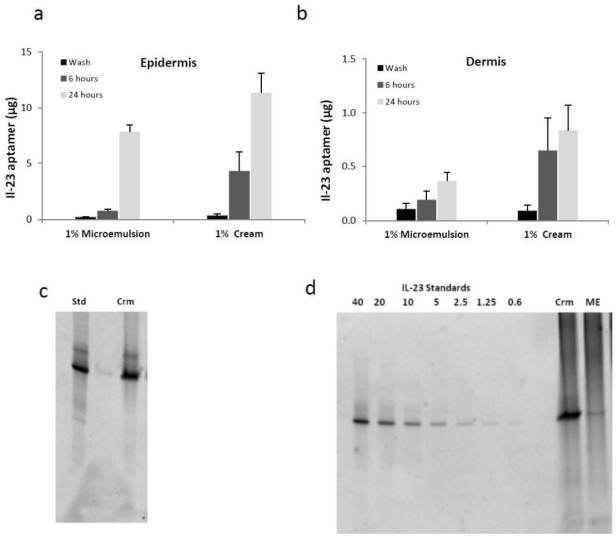

Figure 4. Dual Hybridization Assay demonstrates that topical application of IL-23 aptamer penetrates human skin at therapeutic levels.

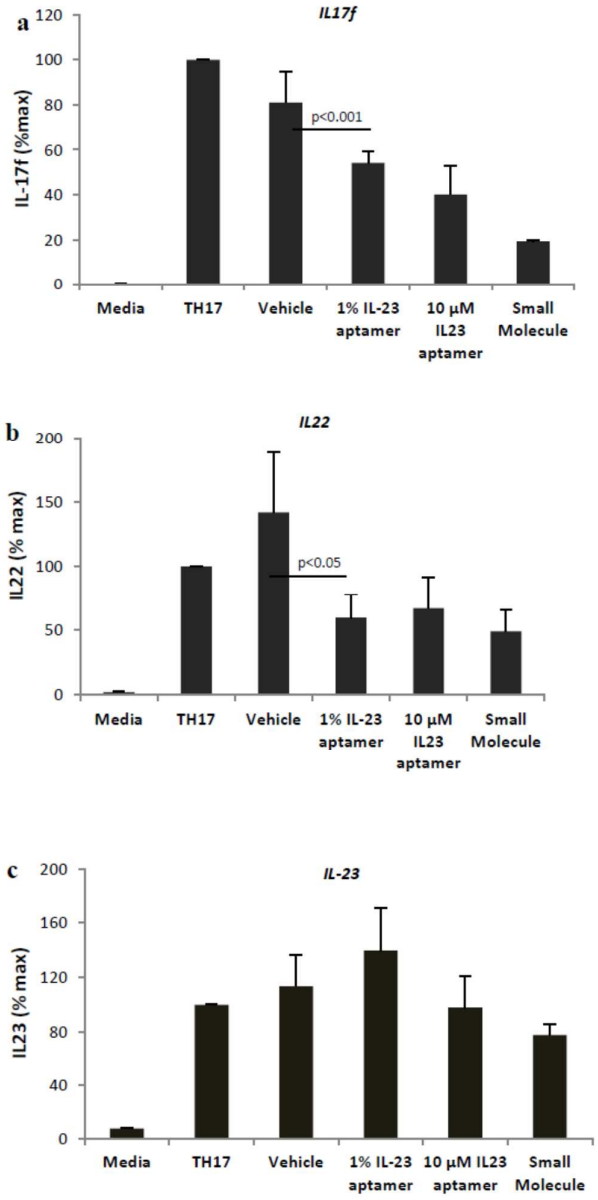

Figure 5. Topical application of IL-23 aptamer inhibits Th17 derived cytokines in human skin.

Supplementary Information. S1

The IL-23 aptamer is biologically active

STAT3 Activity in PHA-Blast cells

Endogenous IL-23 was prepared from the conditioned media of activated purified primary human monocytes by affinity purification. Peripheral Blood Mononuclear Cells (PBMC) were obtained from buffy coats prepared from fresh human blood. Monocytes were isolated by adherence to CD14 coated magnetic beads (Miltenyi, Cologne, Germany). To induce and enhance IL-23 expression, monocytes were treated with LPS and anti-IL-10 blocking antibodies. After 24 hours, conditioned media was collected and frozen. Sepharose NHS agarose beads (Sigma, St. Louis, MI) were coupled with non-neutralizing p19 monoclonal antibodies (eBioscience, San Diego, CA) and incubated overnight with pooled conditioned media from multiple donors. Beads were washed and endogenous IL-23 eluted with acid, and neutralized with a TRIS-base, BSA containing buffer. The eluate was dialyzed with PBS, and the purified protein was aliquoted and frozen. Expression of IL-23 from monocytes was confirmed by testing conditioned media using the p19/p40 enzyme-linked immunosorbent assay (ELISA) from eBioscience (San Diego, CA). The ELISA plate was coated with an anti-p19 antibody and captured antigen was detected with an anti-p40 antibody, thus specifically measuring the IL-23 cytokine. A titration of purified protein was applied to IL-2/PHA activated T-cells for 15 minutes to induce the phosphorylation of STAT3. pSTAT3 (phospho-STAT3) in cell lysates were subsequently measured by ELISA (Cell Signalling Technologies, Danvers, MA). Phosphorylated STAT3 from PHA Blast cells treated with purified endogenous IL-23 was measured by colorimetric ELISA after 15 minutes of stimulation with dialyzed eluate. The endogenous protein was subsequently used in PHA Blast phospho-STAT3 assays at a volume falling in the linear range of the curve. Titration curves were generated using PHA blasts from seven different donors and tested at concentrations between 0.00057 and 500 nM. Seven 12-point titration curves, each in duplicate, were used to calculate a mean (+/- SEM).

Phospho-STAT3 assay

IL-23 aptamer inhibition of endogenous IL-23 activation of PHA/IL-2 activated T- cells was tested by measuring levels of phospho-STAT3. Binding of IL-23 to its receptor on activated T-cells stimulates several STAT pathways, including STAT3. PBMC's from fresh human blood (Archemix) were isolated by centrifugation in a histopaque gradient and treated with PHA/IL-2 to enrich for T-cells and to upregulate IL-23 receptors. Cells were serum starved and treated with endogenous IL-23 for 15 minutes, then lysed. Relative levels of phospho-STAT3 in IL-23 treated lysates, in the presence and absence of IL-23 aptamer or a neutralizing p19 antibody, were measured by ELISA (Cell Signalling Technologies, Danvers, MA). Titrations of aptamer/antibody were used to generate inhibition curves from which the cellular IC50 determinations were made.

Results

Three different cellular assays demonstrated biological activity of the aptamer. (I) Inhibition of IL-23 dependent stimulation of STAT3 activity in PHA-Blast cells showed that both the parent full length IL-23 aptamer (84-mer) and minimer (61-mer) were biologically active (Figure 1a). The parent cellular IC50 was 0.26 nM ± 0.036 nM and the more potent minimized aptamer IC50 was 0.075 nM ± 0.030 nM (Figure 1b). The activity of both aptamers was greater than the control anti-p19 antibody, cellular IC50=0.69 nM ± 0.12 nM. (II) Receptor binding of IL-23 on activated T-cells stimulates several STAT pathways, including STAT3. The ability to block endogenous IL-23 activation in PHA/IL-2 activated T-cells, evaluated by measuring levels of phospho-STAT3, also demonstrated aptamer biological activity; representative anti-p40 antibody and IL-23 aptamer inhibition curves are in Figure 1b. (III) Finally, the ability of the IL-23 aptamer to inhibit IL-12 activation of PHA/IL-2 activated T-cells was evaluated. Similar to IL-23, IL-12 receptor binding on activated T-cells stimulates several STAT pathways, including STAT3 and many IL-23 antagonists also inhibit IL-12 since they share the p40 subunit. The IL-23 aptamer only inhibits IL-23 activation and not IL-12 activation, much like the anti-p19 antibody. Representative p19 antibody and IL-23 aptamer inhibition curves (Figure 1c) show that the IL-23 aptamer is specific for IL-23. From seven 12-point titration curves, each in duplicate, the mean (±SEM) cellular IC50 was 296 ± 90 pM for the IL-23 aptamer (Figure 1d). The IL-23 aptamer has > 500 nM binding affinity to IL-12 as assessed by a radiolabelled dot blot assay.

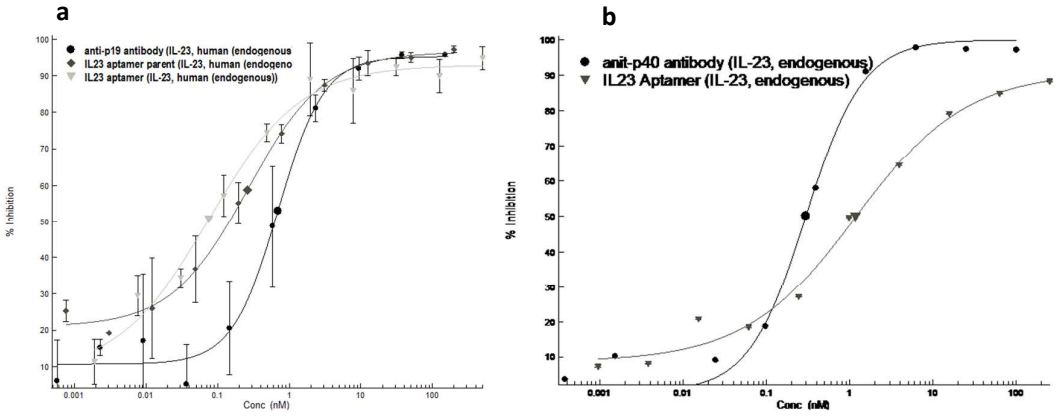

d

IC_{50} (nM)		
Donor	p19	IL-23 Aptamer
1	2.84	0.714
2	8.82	0.075
3	0.088	0.033
4	0.172	0.243
5	0.896	0.271
6	0.426	0.241
7	1.04	0.501
Mean	**2.04**	**0.296**
SEM	1.18	0.09

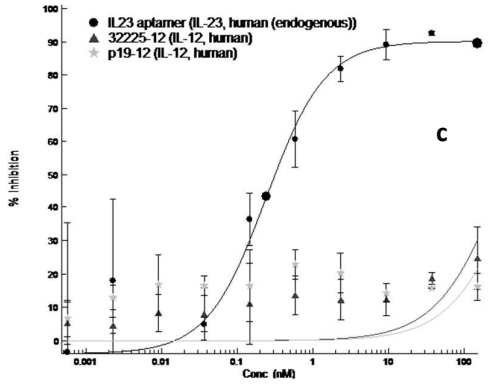

Figure S1. The selection and cellular activity of the IL-23 aptamer. (a) Functional activity following minimization and optimization of the IL-23 aptamer. (b) IL-23 aptamer inhibition of endogenous IL-23 in the PHA Blast phospho-STAT3 assay. (c) Activity of the IL-23 aptamer against eIL-23 and rIL-12. (d) Percent inhibition by p19 neutralizing antibody and the IL-23 aptamer in the PHA Blast phospho-STAT3 assay from individual donors.

Supplementary Information. S2

In vitro selection of IL-23 modified RNA Aptamer

The DNA library consisted of a 40-nucleotide random region (N40) flanked by two constant regions, 5'-GGAGGGAAAAGTTATCAGGC-N_{40}-CGACGAGTAGGCTAGTCTGATGCC-3'. The template was amplified with a primer containing the T7 promoter sequence 5'-GACTGTAATACGACTCACTATAGGAGGGAAAAGTTATCAGGC-3' (underlined portion binds to DNA template). The original library was created by transcribing the double stranded DNA templates as 2'-fluoro and 2'-methoxy modified RNA with a mutant T7 RNA polymerase (Y639) to incorporate the modified nucleotides (mA, mG, fC, and fU residues). The modified RNA library was purified by polyacrylamide gel electrophoresis (PAGE).

The initial selection round contained 10^{14} molecules of library incubated at 37°C for 1 hour with 1 μM of recombinant Interleukin 23 (IL-23, from R&D Systems) in Dulbecco's Phosphate Buffered Saline with calcium chloride and magnesium chloride (DPBS++). Aptamer:pool complex was partitioned using nitrocellulose filter plates pre-treated with 0.5M KOH. Washes used DPBS++ and the selected pools were eluted from filters with urea elution buffer (7M Urea, 100 mM NaOAc, 3 mM EDTA pH 5.7). Eluted modified RNA was reverse transcribed with Thermoscript Reverse Transcriptase (Life Technologies) with the reverse primer, 5'-GGCATCAGACTAGCCTACTCGTCG-3' and amplified by polymerase chain reaction (PCR) with *Taq* polymerase and both forward and reverse DNA primers. PCR product was transcribed using the same T7 RNA polymerase above, gel purified, and put in to the subsequent round. The DNA pools from rounds were cloned into pUC19 and sequenced on an ABI 3730 sequencer to identify N40 DNA sequence of the full length IL-23 aptamer (parent; precursor to IL-23 aptamer).

Supplementary Information. S3

Dual Hybridization Assay

The dual hybridization assay (DHA) has been previously used with plasma and vitreous humour samples (Drolet et al, 2000). This assay is analogous to an ELISA where aptamer is allowed to hybridize to capture and detection DNA oligonucleotide probes. The capture probe (ARC35141; Integrated DNA Technologies) binds to the 13 nucleotides at the 5'-terminus of the aptamer and was covalently attached to magnetic beads via a 3'-terminal amino linker. The detection probe (ARC35156; Integrated DNA Technologies) was complementary to the 15 nucleotides at the 3'-terminus of the aptamer and was biotinylated at the 5'-terminus.

DHA assay plates were prepared by coating 96 well plates with 100 µL of capture probe (250 nM in 1mM EDTA/DPBS) and incubated at 4°C overnight. The capture probe solution was removed and the plate washed with 3 x 300 µL of wash buffer (Tris buffered saline with Tween; TBST) with a minimum of 1 minute soaking time for each of the 3 washes cycles and the plate was tapped out on absorbent paper after each wash. Following removal of wash buffer, 200 µL of blocking solution (5 % w/v BSA in TBST) was added to each well and the assay plate was sealed and incubated at room temperature for 60 minutes on an orbital shaker. The blocking solution was removed and the plate washed as above. A standard curve of aptamer was prepared by doubling dilutions to produce standards from 10 nM to 10 pM and DPBS as a blank sample (0 pM) was added in duplicate (60 µL per well) to a fresh 96 well plate (hybridisation plate). The extracted epidermis and dermis samples were added to the hybridisation plate (60 µL). To each well, 60 µL of the detection probes (150 nM in DPBS) was added. The final concentration of detection probes was 75 nM and aptamer standard concentrations were from 0 pM, 5 nM to 5 pM. The hybridization plate was sealed and placed in an oven at 65°C for 40 minutes to allow the aptamer to hybridise with the probes, and then allowed to cool to room temperature. One hundred µL of the aptamer standard/sample:detection probe mixture was transferred from the hybridization plate to a DHA assay plate, sealed and incubated overnight at 4°C to allow hybridization of the aptamer and capture probes. This assay solution was removed and the plate washed with TBST as above. One hundred µL of the streptavidin-poly-HRP diluted 1:20,000 with DPBS was added to the DHA assay plate, which was then sealed and incubated at room temperature for 1 hour while shaking. The streptavidin-poly-HRP solution was removed and the plate again washed with TBST before 100 µL of the TMB substrate solution (at room temperature) was added to each well; the plates were incubated at room temperature for 5 minutes until sufficient colour developed. Stop solution (100 µL) was added to each well and the plate was read at 450 nm within 30 minutes after stopping the reaction. Data analysis used Prism 5 for each plate, the background A450 value (0 pM aptamer) was subtracted from all values within the sample set. The recovered aptamer (mass per cm^2) was converted to concentration (µmol/L) in each skin layer where the volume of epidermis (cm^3) was assumed to be 0.015 cm^3 and the volume of dermis was assumed to be 0.035 cm^3. The dosing area was 1cm^2.

Supplementary Information. S4

Th17 Stimulated Human Ex-Vivo Skin Model

Cornification media: Media consisted of 237 mL of Dulbecco's Modified Eagle Medium (DMEM) with 4.0 mM L-Glutamine and without CaCl, Glucose, Sodium Pyruvate, and NaHCO3 (Invitrogen, custom order), 237 mL Ham's F-12K (Kaighn's) Medium (Gibco®, 21127-022), 1 mL 90mM Adenine, 1mL 0.94M CaCl, 1 mL 10nM Tri-iodothyronine, 1 mL Insulin-Transferrin-Selenium-Ethanolamine (ITS -X) (100X) (Gibco® 5100-056), 5 mL Antibiotic-Antimycotic (100X) (Gibco® 15240-062), 10 mL Foetal Bovine Serum (FBS) (HyCloneTM, SH30071.01HI), 5 mL GlutaMAX™ Supplement (Gibco®, 35050-061), 0.1 mL 50mg/ml Gentamicin (Invitrogen, #15750060).

Th17 Stimulation Cocktail: The cytokine cocktail was optimized to stimulate skin resident immune cells to release TH17 associated cytokines, including IL-17f and IL-22, as previously described 16. Briefly, skin was stimulated with a combination of 1 µg/ml purified NA/LE Mouse anti-human CD3 (BD Pharmingen, Cat# 555329) and 2 µg /ml anti-human CD28 (R&DSystems, Cat# MAB342), 1 µg /ml anti-Human IFN-gamma Antibody (R&DSystems, Cat#MAB2851), 1 µg/ml anti-Human IL-4 Antibody (R&DSystems, Cat# MAB304), 10 ng/ml Recombinant Human (rh) IL-1b/IL-1F2 (R&DSystems, Cat# 201-LB-025/CF), 10 ng/ml rhIL-6 (R&DSystems, Cat# 206-IL-010/CF), 1 ng/ml Recombinant Human TGF-b1 (R&DSystems, Cat# 240-B-010/CF), and rh IL-21 (Southern Biotech, Cat# 19000-00). All components were incorporated in a single mixture with the cornification media.

Tissue culture using Static Cells: Freshly excised healthy human skin was dermatomed to 750 µm and cleaned with antibiotic/antimycotic solution made up as 1% Gibco™ Antibiotic-Antimycotic (100X), 0.1% Gentamicin in 1x Dulbecco's Phosphate Buffered Saline. Twelve mm diameter biopsies were cut using disposable single-use biopsy punches (Acupunch, Acuderm, Inc) and washed in antibiotic/antimycotic solution for 5-10 minutes. Skin biopsies were placed on autoclaved 7 mm (0.38 cm^2) unjacketed static cells with 2 mL receptor volume (PermeGear, Inc; No. 6G-01-00-07-02) and a leak proof seal was maintained using metal clamps and donor chamber. The receptor chamber was filled with cornification media. Static cells were then placed in a humidified incubator at 37°C and cultured as previously described (Smith et al, 2016). First, test articles were dosed topically or systemically in the media and twenty-four hours later, the media was replaced and the Th17 stimulation cocktail was added to the receptor chamber of the Franz cells. Twenty-four hours after stimulation, the tissue was harvested, minced to less than 1x1x1 mm pieces and stored in 10x volume of RNA later (Qiagen, Cat# 76104) with 300 µL of RNeasy Lysis Buffer (Qiagen, Cat#79216) supplemented with 1% 2-Beta-Mercapto-Ethanol for RNA isolation.

Small Molecule Control: A ROR gamma inverse agonist (MW=476 g/moles) was used as a positive control at 10 µM in cornification media based on its known positive activity in the Th17 stimulated human *ex vivo* skin model (Smith et al, 2016).

RNA Isolation & Quantitation: Approximately 40 mg of minced tissue was added to homogenization tubes containing 2.8 and 1.4 mm ceramic beads. The tissue was disrupted

using a high-throughput bead mill homogenizer (Precellys®24 Atkinson, NH) at 6300 rpm for 30 seconds and 10 cycles with a 2-minute ice break. The homogenate was digested by adding 490 µL of water containing 10 µL Proteinase K (Thermo Scientific, Cat # E00491) at 55°C for 15 minutes. Digested tissue was spun down for 3 minutes at 10,000x g to pellet cell debris and the supernatant was used for RNA isolation using Qiagen's Mini RNA Isolation kit (Cat # 74106) according to the manufacturer's protocol. Total RNA was quantified using a Nanodrop 2000 (Thermo Scientific, Wilmington, DE). Isolated RNA (1.4µg) from skin tissue was used as a template in a 20 µL PCR volume using an Invitrogen SuperScript VILO cDNA Synthesis kit (# 11754-050) to create a cDNA template. The cDNA was diluted 1:25 for subsequent qPCR with the specific TaqMan probe for each gene to be quantified. A Life Technologies AVii7 PCR machine was used for the qPCR 40 amplification cycles. RNA levels of GAPDH, IL-17a, IL-17f and IL-22 relative expression were calculated using the ΔΔCT method.